SPONTANEOUS NEUROTRANSMISSION AS A DRIVER OF CALCIUM SIGNALING

APPROVED BY SUPERVISORY COMMITTEE

_____

_____

_____

_____

DEDICATION

I would like to thank my parents, who have supported my academic endeavors longer than anyone.

SPONTANEOUS NEUROTRANSMISSION AS A DRIVER OF CALCIUM SIGNALING

by

AUSTIN LOWELL REESE

DISSERTATION

Presented to the Faculty of the Graduate School of Biomedical Sciences

The University of Texas Southwestern Medical Center at Dallas

In Partial Fulfillment of the Requirements

For the Degree of

DOCTOR OF PHILOSOPHY

The University of Texas Southwestern Medical Center at Dallas

Dallas, Texas

December, 2016

NMDA RECEPTORS UNIQUE TO SPONTANEOUS NEUROTRANSMISSION DRIVE POSTSYNAPTIC CALCIUM SIGNALING TO MAINTAIN SYNAPTIC HOMEOSTASIS

Publication No. 3

Austin Lowell Reese, PhD

The University of Texas Southwestern Medical Center at Dallas, 2016

Supervising Professor: Ege Taner Kavalali, PhD

Spontaneous neurotransmission is a stochastic mode of neurotransmitter release that is not coupled to action potential arrival at the presynapse. Recent evidence has shed light upon the presynaptic and vesicular fusion machinery that makes this mode of release unique to action potential driven, or evoked release, yet the postsynaptic reception of these differing signals has yet to be probed in detail. Here, I illustrate that evoked and spontaneous release modes coexist within the same synapses, yet the neurotransmitter released falls upon separate subsets of postsynaptic receptors. As a consequence of this phenomenon, in glutamatergic hippocampal synapses the NMDA receptors activated by spontaneous release are able to

drive large calcium transients that maintain synaptic homeostasis and suppress local protein synthesis.

TABLE OF CONTENTS

PRIOR PUBLICATIONS

Bal, M., J. Leitz, A. L. Reese, D. M. Ramirez, M. Durakoglugil, J. Herz, L. M. Monteggia and E. T. Kavalali (2013). "Reelin mobilizes a VAMP7-dependent synaptic vesicle pool and selectively augments spontaneous neurotransmission." Neuron 80(4): 934-946.

Reese, A. L**.** and E. T. Kavalali (2015). "Spontaneous neurotransmission signals through store-driven Ca2+ transients to maintain synaptic homeostasis." Elife 4.

LIST OF FIGURES

LIST OF APPENDICES

LIST OF DEFINITIONS

Mini – a spontaneous neurotransmission event; miniature because its current and voltage measurements are small compared to action potential driven transmission

Evoked release – quantal release of neurotransmitter from the presynaptic cell caused by arrival of an action potential and depolarization of the presynaptic compartment

Spontaneous Release – quantal release of neurotransmitter from the presynaptic cell that is not caused by the arrival of an action potential

SNARE – soluble N-ethylmaleimide-sensitive factor–attachment protein receptor

VAMP – Vesicle Associated Membrane Protein

VAMP2 – synaptobrevin2

At rest – resting membrane potential

Resting conditions – conditions where action potentials are absent

ROI – region of interest

Puncta – in microscopy, a small, distinct point of fluorescence

MK-801 - (+)-5- methyl-10,11-dihydro-5H-dibenzo[a,d]cyclohepten-5,10-imine maleate

mEPSC – miniature excitatory postsynaptic current

eEPSC – evoked excitatory postsynaptic current

Drosophila – *Drosophila Melanogaster*, the common fruit fly

NMJ – neuromuscular junction, the nerve terminal where transmitter is released onto muscle fibers to stimulate muscle contraction

R_p – (evoked) response probability

VGCC – Voltage-Gated Calcium Channel

LVA – Low Voltage Activated (calcium channels)

HVA – High Voltage Activated (calcium channels)

NMDA - N-Methyl-D-aspartic acid, the agonist for which the NMDA receptor is named

AMPA - α-amino-3-hydroxy-5-methyl-4-isoxazolepropionic acid, the full agonist of the AMPA receptor

mGluR – metabotropic glutamate receptor, a G protein coupled class of receptors (with the exception of mGluR

G protein - guanine nucleotide-binding proteins

LTP – long term potentiation, a high activity dependent strengthening of a synapses electrical signaling

LTD – long term depression, weakening of synaptic strength due to repeated low activity patterns

PLC – phospholipase C, a membrane bound enzyme that cleaves PIP_2 into IP_3 and DAG

PKC – protein kinase C, a Ca^{2+} dependent kinase

PIP_2 – phosphatidylinositol 4,5-bisphosphate, a modified membrane phospholipid

IP_3 – inositol 1,4,5-triphosphate, the soluble head group cleaved by PLC

DAG – diacylglycerol, a membrane bound lipid which activates PKC

CaM – calmodulin, a soluble Ca^{2+} binding protein that acts as a Ca^{2+} dependent effector for many other proteins

CICR – Ca^{2+}-induced Ca^{2+} release

RyR – ryanodine receptor

ER – endoplasmic reticulum

RARα – retinoic acid receptor α

CHAPTER ONE
Introduction to Spontaneous Neurotransmission

EVIDENCE FOR THE SEPARATION OF MINATURE AND EVOKED RELEASE IN THE PRESYNAPTIC COMPARTMENT

Though the action potential was discovered in 1848, it was not until 1952 that minis were first described in the laboratory of Bernard Katz (Rothschuh 1973). In this first publication, the authors were recording with sharp electrodes in an exposed muscle preparation. They discovered that when recording voltage in the muscle fiber near the terminal end of the nerve they could see small, spontaneously arising, positive voltage transients. In this first description, the authors deduced several critical facts about this phenomenon. First, the excitatory potentials were generated by the nerve, and could not be recorded further down the muscle fiber. Second, the spontaneous potentials were too large to be generated by a single ion channel opening. This means that the potentials were due to several channels opening at once, and must be due to quantal transmitter release rather than neurotransmitter diffusion. Finally the authors noted that by their calculation, thermal voltage noise at the nerve terminal would not cause sufficient depolarization to release vesicles by the same mechanism that an action potential would (Fatt and Katz 1952).

These findings immediately raised a multitude of questions about the nature of synaptic transmission and the function of minis. If neurons communicate information using the action potential, why would they spontaneously generate signals are essentially noise? Is neurotransmitter release an inherently stochastic system, or do action potential evoked

release and spontaneous release utilize separate mechanisms? In the following dissertation, I will present both published literature and experimental evidence to propose that evoked and spontaneous release are molecularly distinct both at the presynapse and postsynapse, and that minis convey a critical maintenance signal that the postsynaptic cell utilizes in balancing its activity patterns.

SNARE proteins designate synaptic vesicles for spontaneous release

SNARE proteins are helical proteins that coil together facilitate the fusion of membrane compartments by bringing the membranes into contact; in this case synaptic vesicles with the presynaptic plasma membrane. T-SNARES reside on the plasma membrane and the complimentary v-SNARE on the vesicle surface. The canonical SNARE complex for evoked vesicle fusion includes the v-SNARE VAMP2 and the t-SNAREs SNAP25 and syntaxin-1 (Weber, Zemelman et al. 1998). The majority of vesicle fusion involves these core proteins and spontaneous release has been shown to use this core complex, but does not require it exclusively. In SNAP-25 null neurons, there is a ~60% reduction in spontaneous release frequency, yet minis persist using alternative SNARE proteins (Tafoya, Mameli et al. 2006, Reese and Kavalali 2015). Fast synchronous evoked release, however, does not share this same flexibility. SNAP25 knockout animals are not viable and exhibit no evoked neurotransmitter release (Washbourne, Thompson et al. 2002). The v-SNARE VAMP2 is also critically involved in evoked transmitter release. In VAMP2 null mice, action potential stimulation produces virtually no response, yet spontaneous activity again persists but at

roughly 15% the normal frequency (Schoch, Deak et al. 2001). In imaging studies, VAMP2 was shown to be a ubiquitous component of spontaneously fusing vesicles and readily trafficks from vesicle to the plasma membrane in the absence of stimulation (Ramirez, Khvotchev et al. 2012). However, as the knockout animal illustrates it is not required as in its absence, alternative SNARE combinations are in use.

Though evoked release machinery seems to require specific components, there are tens of SNARE proteins that localize to presynaptic compartments and are found on synaptic vesicles (Takamori, Holt et al. 2006). In particular, the two v-SNARE proteins Vti1a and VAMP7 designate vesicles to traffic spontaneously (Ramirez, Khvotchev et al. 2012). To study this, fusion proteins of the SNARE in question were made with the pH sensitive GFP, pHluorin or its red shifted variant pHtomato. These constructs place the pH sensitive GFP in the acidic lumen of the synaptic vesicle where the fluorescence is quenched. Upon fusion with the plasma membrane, the fluorescent tag becomes visible. Using this molecularly specific assay for vesicle fusion, it was found that while Vti1a and VAMP7 only trafficked to the plasma membrane sparingly in response to stimulation they readily trafficked spontaneously. Incomplete knockdown of these two proteins in cell culture produces a distinct reduction in minis that occur with short inter-event intervals while producing no discernible impact on evoked release.

Spontaneously fusing vesicles are functionally distinct from evoked vesicles

Identification of proteins that preferentially facilitate spontaneous vesicle fusion over evoked fusion brings about the idea that vesicles may belong to discrete groups or pools. In fact, this idea is functionally well established as it has been observed for some time that under multiple types of stimulation, some number of vesicles will remain in the presynaptic compartment that are reluctant to fuse in response to action potentials (Rosenmund and Stevens 1996, Fredj and Burrone 2009). In fact, spontaneously cycling vesicles can be functionally separated from evoked vesicles as individual synaptic vesicles undergo repeated cycling during neurotransmission. Once a vesicle fuses with the target membrane at the active zone, it dumps its contents into the synaptic cleft. The vesicle is then endocytosed and refilled with neurotransmitter for reuse (as reviewed in Sudhof 2004). While the vesicle is integrated into the plasma membrane, membrane anchored proteins previously held in the vesicle lumen are exposed to the extracellular solution.

Taking advantage of this fact, lipophilic fluorescent dye can be loaded onto the plasma membrane where it is incorporated into vesicles upon endocytosis. Upon washing the remaining dye off the plasma membrane, the dye on synaptic vesicles remains and its fluorescent signal decreases as vesicles once again fuse with the now unlabeled plasma membrane. Using this technique, the signal at synapses that were labeled during spontaneous activity was destained very slowly if cells were stimulated to release evoked vesicles. In contrast, dye that was taken up during evoked activity was readily recycled to the plasma membrane upon a second round of stimulation. These results strongly suggest that vesicles are unique to each mode of release and maintain their identity even after undergoing fusion (Sara, Virmani et al. 2005).

Complexin as specialized regulator of spontaneous release

Once assembled, the 4 helix bundle of v-SNARE and t-SNARE proteins interact with multiple proteins including the Ca^{2+} sensors of the synaptotagmin family and proteins of the complexin family. As an action potential arrives at the presynapse, the rise in membrane voltage serves to open voltage-gated Ca^{2+} channels which flood the presynaptic compartment with calcium ions. In evoked transmission, synaptotagmin-1 and in some brain regions, synaptotagmin-2 (Marqueze, Boudier et al. 1995) sits bound to the SNARE complex awaiting this Ca^{2+} influx; acting as the Ca^{2+} sensor that triggers fusion. Cells lacking synaptotagmin-1 are entirely deficient in fast synchronous evoked release, yet display an increase in mini frequency compared to control animals (Kerr, Reisinger et al. 2008). The differential action of synaptotagmin-1 on the two modes of release can largely be explained by the action of complexins 1 and 2. Much like the phenotypes in synaptotagmin-1 knockout neurons, a double knockout of the soluble complexins 1 and 2 produces a deficit in evoked release and an increase in mini frequency (Yang, Cao et al. 2013). Complexins bind to SNARE complexes by placing their main α-helix in line with the 4 helix bundle of the SNARE complex leaving a second α-helix and the N terminus free (McMahon, Missler et al. 1995, Tang, Maximov et al. 2006). Once bound, complexin has two roles. Firstly, its binding serves to prevent the SNARE complex from fusing the two membranes. This action is thought to account for its negative regulatory action on spontaneous release. Once complexin is bound, in order for the vesicle to fuse complexin must be displaced by Ca^{2+} bound synaptotagmin-1. These traits account for its differential effects as it both prevents Ca^{2+}

independent fusion and promotes Ca^{2+} dependent vesicle fusion (Jorquera, Huntwork-Rodriguez et al. 2012). Second, complexin changes the conformation of the SNARE complex to ready it for fusion, and thus plays a role in preparing the vesicle for fast synchronous release; thereby allowing the vesicle to fuse the instant the Ca^{2+} signal arrives (Maximov, Tang et al. 2009). Taken together, the above results provide evidence that spontaneous neurotransmission not only uses a molecularly and functionally distinct set of vesicles but the presynaptic machinery possesses the molecular mechanism to independently control the two forms of release through the actions of complexin.

EVIDENCE FOR SEPARATION OF EVOKED AND SPONTANEOUS SIGNALS IN THE POSTSYNAPTIC COMPARTMENT

If the presynapse is organized in such a way that spontaneous and evoked release are unique modes of signaling, this brings into question the way in which the postsynaptic cell might interpret each type of neurotransmission. Without making further assumptions, its logically possible that evoked and spontaneous release could be separated spatially and activate different receptors or perhaps temporally, acting through the same receptors at different times. In 2006, the signaling importance of spontaneous neurotransmission was starting to become clearer (discussed in chapter 5), but the question of whether minis signaled through the same receptors as evoked release remained unaddressed. A 2008 publication authored by Deniz Atasoy in the Kavalali lab addressed exactly this question.

The underpinnings of this study relied on the pharmacokinetics of the drug MK-801, a selective NMDA receptor antagonist that binds the open conformation of the channel. This

property makes the drug use-dependent, as the channel needs to be opened before the drug can bind, and remains blocked unless the drug is washed out. Using this quirk, Dr. Atasoy cut acute hippocampal slices and could separate spontaneous and evoked receptor activation by selectively applying the drug. If the drug was applied in the absence of stimulation, mini frequency ran down to nearly nothing over the course of 10 minutes. However, when comparing evoked responses before and after MK-801 treatment there was only a 15% decrease in EPSC amplitude. This limited crossover of the receptors activated by evoked and spontaneously released glutamate held true in the inverse experiment as well. In high-density hippocampal cultures, minis were recorded before and after stimulating in the presence of MK-801 which revealed no significant difference in the mEPSC amplitude (Atasoy, Ertunc et al. 2008).

If the receptors that receive spontaneous glutamate are spatially separated from those that receive evoked glutamate, there are two logical possibilities. First, the receptors could be separated at unique synapses. The implications of this hypothesis would be that specialized spontaneous-only synapses exist and signal through postsynaptic machinery that is physically separated from evoked synapses along the dendrite. Taking into consideration that previous single synapse resolution dye loading experiments and additional pHluorin experiments conducted by Dr. Atasoy showed both evoked and spontaneous vesicle trafficking within the same fluorescent puncta, this possibility would be surprising. The alternative hypothesis would be that spontaneous and evoked release occur at the same synapse, but are separated spatially such that the receptors for each do not intersperse. A computational model created by Dr. Atasoy proposed that due to the relatively slow diffusion constant inside the synaptic

cleft and the relatively lower open probability of receptors for evoked release (which resist saturation at higher stimulation frequencies) it is theoretically possible for a 0.36 μm^2 synapse to accommodate separated signals.

The question of how spontaneous and evoked release are postsynaptically distinguished was first addressed by Dr. Troy Littleton's group at MIT in a *Drosophila* neuromuscular junction preparation. The NMJ is a large nerve terminal structure that forms boutons over the muscle fiber with many individual active zones. Unlike mammals where acetylcholine is the neurotransmitter of choice, *Drosophila* NMJs release glutamate. The authors utilized a GCaMP5 with a myristoylation tag (myrGCaMP5) that they expressed in muscle cells. The myristoylation tag localized the Ca^{2+} sensitive GFP to the plasma membrane, where it was most sensitive to Ca^{2+} influx. Imaging with a spinning-disk confocal microscope, they were able to visualize the Ca^{2+} influx from both spontaneous and evoked responses. Identification of functional active zones was validated by comparing their recordings to a post-hoc immunostain for the active zone protein bruchpilot.

Using this experimental system, the authors showed that while both spontaneous and evoked release were evenly distributed across the end plate, there tended to be clusters of active zones with higher spontaneous release frequencies. Furthermore, the Poisson distribution does not describe the distribution of spontaneous release rates and thus spontaneous release events are not fully independent of one another at the single synapse level. When comparing evoked to spontaneous release rates at single synapses, the authors measured that roughly 41% of measured active zones responded spontaneously and in response to stimulation, 36% only responded to stimulation, and 22% responded

spontaneously only. It is somewhat difficult to make concrete assessments about the active zones that did not display dual release mode activity as the recording window was 5 minutes or less and these active zones may represent very low release rates rather than none at all. However, these results clearly illustrate at least some amount of overlap in release modes at single active zones in the fly NMJ (Melom, Akbergenova et al. 2013).

A second and more recent study has taken a similar approach to studying release modes in the fly NMJ yet coming to very different conclusions. Dr. Ehud Isacoff and his research group at the University of California, Berkeley came across similar findings as Atasoy et al. by using philanthotoxin, a use-dependent blocker of the muscle glutamate receptors. In their preparation, stimulation but not spontaneous neurotransmission could progressively block evoked responses in a before and after experiment. Using a similar, targeted GCaMP imaging approach as the Littleton group (but notably, in a different muscle of the same segment), the Isacoff group imaged both stimulated and spontaneous responses, finding very little spatial overlap. Comparing spontaneous release rates and evoked release probability of individual active zones yielded an inverse relationship where certain active zones preferred one mode or the other (Peled, Newman et al. 2014).

While I believe each groups observations to be correct in their respective systems, the significance of either study is not easily interpreted in the context of mammalian central synapses which do not share the same molecular or ultrastructure as the fly NMJ. The experiments outlined in chapter 2 directly address these questions in a mammalian model system.

CHAPTER TWO

Experimental Evidence for the Postsynaptic Separation of Evoked and Spontaneous Neurotransmission

INTRODUCTION

The vast majority of neuronal subtypes in the mammalian central nervous system exhibit both action potential (AP) synchronized evoked neurotransmitter release and stochastic, spontaneous neurotransmitter release. Previous work by our group and others have shown that spontaneous neurotransmission is critical in the homeostatic regulation of synaptic strength which may have implications for the efficacy of novel antidepressants (Sutton, Ito et al. 2006, Nosyreva, Szabla et al. 2013, Gideons, Kavalali et al. 2014). In particular, our work has shown that the Ca^{2+} dependence of these effects is driven by the NMDA receptor via a ryanodine receptor mediated coupling to Ca^{2+} stores in the endoplasmic reticulum (Reese and Kavalali 2015). An early investigation into the possibility that evoked and spontaneous neurotransmission may be separated spatially found that glutamate from evoked neurotransmitter release fell upon a subset of NMDA receptors distinct from those activated by spontaneous neurotransmission (Atasoy, Ertunc et al. 2008). However, these results did not distinguish between the possibilities that the two modes of neurotransmission may be separated between synapses or within synapses.

More recent experiments in the *Drosophila* neuromuscular junction have come to mixed conclusions about the propensity of a single active zone to participate in both evoked and spontaneous transmission; finding either considerable overlap with a population of spontaneous only active zones or limited overlap with a negative correlation between the two

modes (Melom, Akbergenova et al. 2013, Peled, Newman et al. 2014). To date, no such measurement has been made in mammalian synapses. Here, we utilize the genetically encoded Ca^{2+} sensor GCaMP6f-PSD95 to image neurotransmission at individual synaptic regions to measure the amount of transmission mode overlap in hippocampal neurons.

RESULTS

Visualization of AP5 sensitive postsynaptic Ca^{2+} transients with GCaMP6f-PSD95

In order to detect Ca^{2+} signals in the postsynaptic compartment, we utilized the postsynaptically targeted indicator GCaMP6f-PSD95. This fusion protein is comprised of the fast kinetic variant of the genetically encoded Ca^{2+} sensor GCaMP6 and the postsynaptic scaffolding protein PSD95. Dissociated hippocampal cultures DIV 14-16 were transfected using Lipofectamine 3000 (Thermo Fisher, Waltham MA) to produce sparse cell labeling (<1% efficiency). The indicator was expressed and trafficked to the postsynaptic compartment where it produced punctate signals consistent with a synaptic localization (Figure 2.1A). Images were collected at 5 frames per second which provided sufficient temporal resolution to define individual transients when collecting traces from 2.5 μm regions of interest (ROIs) (Figure 2.1B). In order to maximize NMDA receptor conductance and thus the expected postsynaptic Ca^{2+} signal, cells were imaged in Mg^{2+} free solution (Jahr and Stevens 1990). To determine if the observed transients were in fact NMDA currents, we recorded cells for 4 minutes in Tyrode's solution containing 1 μM TTX and then TTX + 50 mM AP5. The addition of AP5 produced a 98.3% reduction in detected events over 4

minutes which is consistent with the recorded signals originating from postsynaptic NMDA currents.

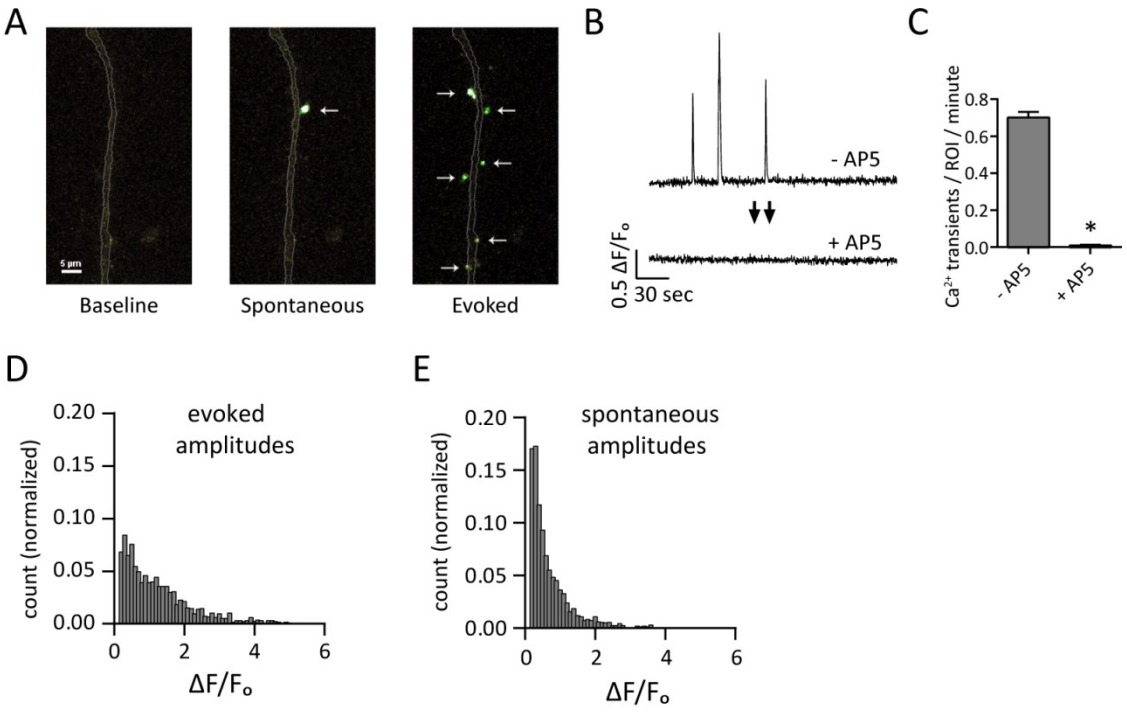

Figure 2.1 – Detection of postsynaptic Ca^{2+} transients with GCaMP6f-PSD95

A. Example images showing a section of dendrite (gray outline) during baseline fluorescence, peak fluorescence of a spontaneous event, and peak fluorescence of stimulus evoked events. Arrows indicate postsynaptic signals. **B.** Example traces from a GCamp6f-PSD95 puncta before and after AP5 treatment. **C.** Quantification showing Ca^{2+} transients detected in TTX before and after the addition of AP5. N = 600 ROIs from 6 experiments, 2 cultures, $p < 0.001$ via students paired T-test. **D.** Amplitude histogram comprised of 1376 Ca^{2+} transients evoked by stimulation. Amplitudes displayed as change in fluorescence between baseline and peak divided by baseline ($\Delta F/F_o$). **E.** Amplitude histogram comprised of 1683 spontaneous events in the same ROIs as D. For figures D-E, N = 250 ROIs from 5 cells and 3 cultures.

Spontaneous response rate and evoked response probability do not correlate at the single synapse level

In response to stimulation with 30 mA of current through a 3 mm spaced bipolar electrode, individual puncta responded in a stochastic manner consistent with the evoked release of synaptic vesicles. To allow recording of both evoked and spontaneous responses, cells were perfused with Tyrode's solution containing 5 μM NBQX, 5 μM muscimol and 20 μM ryanodine. The AMPA receptor antagonist NBQX and the $GABA_a$ agonist muscimol function to prevent spontaneous action potentials and reverberatory network activity during stimulation. Ryanodine was included to block efflux of Ca^{2+} from the endoplasmic reticulum which we have previously shown to contribute to synaptic Ca^{2+} measurements (Reese and Kavalali 2015).

To assess if spontaneous response rate and evoked response rate may be functionally correlated, cells were recorded for 8 minutes during which single action potentials were stimulated every 30 seconds for a total of 15 action potentials. Signal peaks detected within 1 second of a stimulus were considered to be evoked, and all peaks falling out of the 1 second window were considered to be spontaneous in origin (see methods).

Plotting the spontaneous response rate against the evoked response rate for each synapse reveals no linear correlation between the two parameters. A fit line describes a trend towards lower spontaneous response rates in high evoked R_p ROIs, but with very weak correlation ($y = -0.43x + 0.95$, $R^2 = 0.038$). Interestingly, there is a large population of ROIs,

~22%, that exhibit spontaneous but not evoked responses during the recording period. These ROIs may represent synapses that exclusively release spontaneous vesicles, or have a very low evoked R_p (Figure 2.2b, along y axis). The presence of these ROIs suggests that a population of synapses may exist which exclusively signal spontaneously rather than by action potential driven electrochemical neurotransmission. The distribution of observed frequencies for spontaneous responses shows clustering around a mean rate of 0.79 events / ROI / minute with a long right-handed tail (Figure 2.2A). Evoked responses show a much more even distribution with a mean R_p of 0.37 (Figure 2.2C). Similarly, spontaneous response amplitudes exhibit a much more narrow distribution than evoked response amplitudes (Figure 2.1D-E). In addition, we found that neither evoked R_p or spontaneous response rate vary with their straight-line distance to the soma (data not shown).

Previous studies have shown that the distribution of spontaneous synaptic responses in time is not consistent with the events being independent at the population or single-synapse level and thus do not follow the Poisson distribution (Abenavoli, Forti et al. 2002, Melom, Akbergenova et al. 2013). As compared by the χ^2 test, neither the Poisson distribution matching the measured average ($\lambda = 6.2$, $p << 0.001$, excluding zeros, not shown) or the theoretical best fit Poisson ($\lambda = 4.3$, $p << 0.001$, excluding zeros) describe the measured distribution. We therefore conclude that there are one or more constraints on the frequency of spontaneous responses.

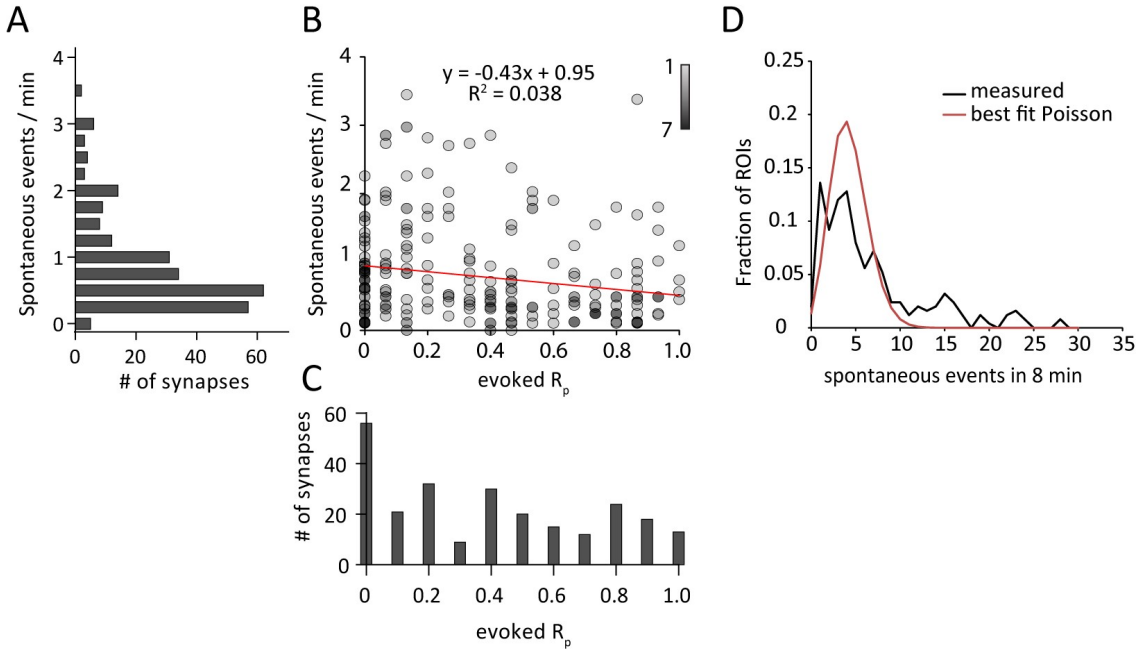

Figure 2.2 – Spontaneous response frequency and evoked response probability show little correlation within the synapse.

A. Histogram showing spontaneous event rates per minute for 250 ROIs from 5 cells and 3 cultures. **B.** Scatter plot of evoked release probability (R_p) vs spontaneous response rate for the same 250 synapses. **C.** Histogram showing the distribution of evoked response probabilities. **D.** Distribution of ROIs by events per 8 minutes plotted with Poisson best fit.

Use-dependent NMDAR block reveals sub-synaptic separation of evoked and spontaneous signals

The noncompetitive, use-dependent NMDA receptor blocker, MK-801 has previously been utilized illustrate that spontaneous and evoked glutamate signals fall upon different subpopulations of NMDA receptors (Atasoy, Ertunc et al. 2008). However, these measurements are electrophysiological or measured population responses rather than quantal single-synapse responses. To investigate whether it is possible to block spontaneous signals

without blocking evoked signals within a single synapse, we stimulated cells with 10 single stimuli, 10 seconds apart to establish a baseline R_p before washing in 10 μM MK-801 for 10 minutes. With MK-801 still in the bath solution, cells were again stimulated 10 times, 10 seconds apart to test for post-treatment responses (Figure 2.3A, bottom). To account for photobleaching and cellular run-down during this long recording period, control experiments were performed without MK-801 (Figure 2.3A, top). During the MK-801 treatment, spontaneous response rate decreased by 87% over 10 minutes ($p = 0.009$ comparing first and last minute with student's T-test). In contrast, there was no significant decrease in spontaneous response rate in the control experiments when comparing the first and last minute ($p = 0.78$, student's t-test) (Figure 2.3B).

In control cells, of the ROIs that responded one or more times during the first stimulation, spontaneous responses were observed in 74% of those ROIs and 47% responded to stimulation after the 10 minute control wash. In the MK-801 treated cells, of the ROIs that responded during the first stimulation, 75% responded spontaneously and 66% responded after treatment. We expect that if spontaneous MK-801 block was blocking a large number of both spontaneous and evoked responding NMDA receptors, there would be a steep decrease in the number of synapses that respond to evoked stimulus after MK-801 treatment. However, the ability of ROIs to respond to evoked stimulus after MK-801 treatment is unaffected compared to control (Figure 2.3C, $p = 0.39$ via one-way ANOVA). These results are consistent with the findings in Figure 2.2 in that the vast majority of ROIs exhibit both spontaneous and evoked responses. Still, the inability of MK-801 to block evoked responses

in ROIs that show both modes of response belies a separation of the two within the same ROI.

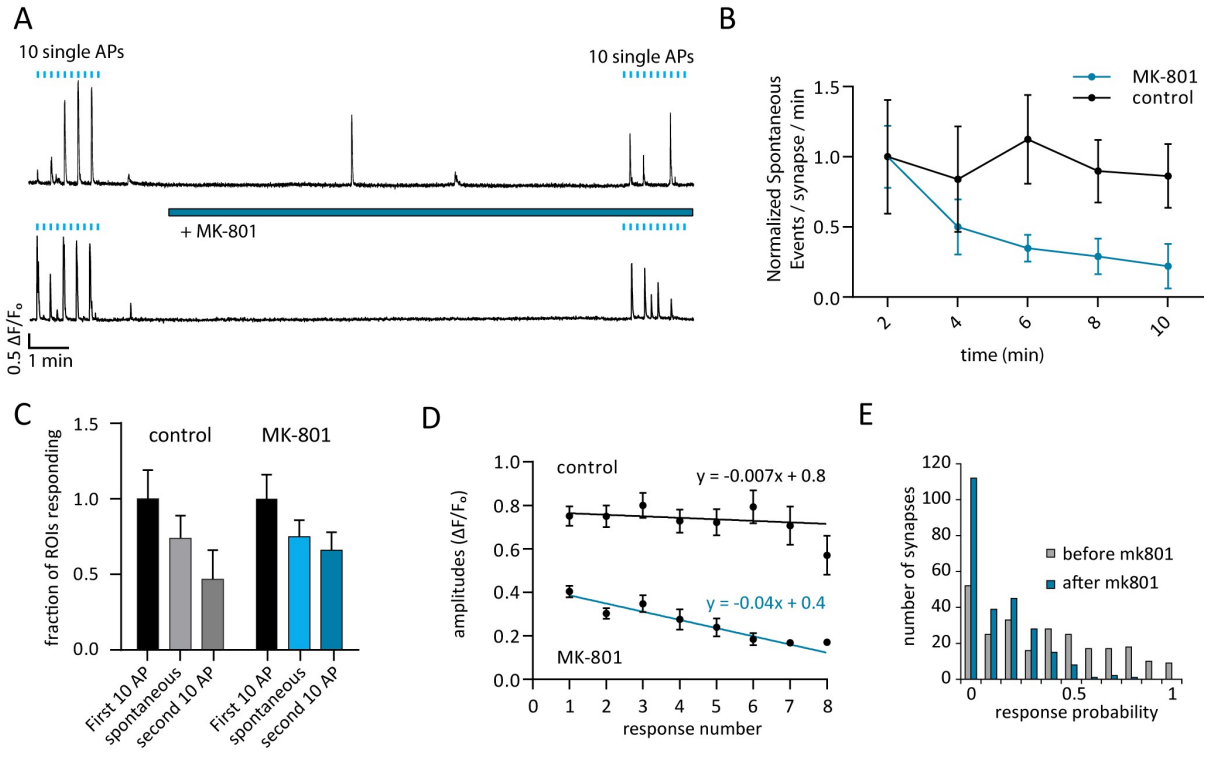

Figure 2.3 – Use-dependent NMDAR blocker MK-801 can selectively silence spontaneous signals without effecting evoked responses within the same synapse.

A. Example traces outlining the experiment with (top) and without (bottom) MK-801 treatment. 10 action potentials were evoked, 10 seconds apart. 4 minutes later, perfusion was changed to Tyrode's solution containing 10 µM MK-801 or vehicle. After 10 minutes in this solution, 10 additional action potentials are evoked, 10 seconds. **B.** Plot shows normalized spontaneous event frequency over the 10 minute treatment with MK-801 or control solution. For MK-801 N = 250 ROIs from 5 cells and 2 cultures. For the control condition, N = 200 ROIs from 4 cells and 4 cultures. **C.** Bars show synapse counts as percent of synapses that respond to the first stimulation in control and MK-801 treated cells. **D.** Average amplitudes as $\Delta F/F_o$ for each response in order per synapse. Initial 10 event averages are taken from control and MK-801 treated cells. For both groups, fit line generated via linear least squares method. **E.** Histogram showing distribution of evoked response probabilities in cells before and after MK-801 treatment.

High spontaneous response rate does not predict magnitude of evoked MK-801 block

During the course of stimulation there was a decrease in amplitude with every subsequent response greater in the MK-801 treated cells compared to untreated. No single ROI responded more than 8 times with MK-801 in the bath solution (Figure 2.3D). This decrease in amplitude is accompanied by a decrease in R_p after MK-801 treatment that preferentially affects high responding ROIs (Figure 2.3E).

Comparing the spontaneous rate measured before the addition of MK-801 against the change in evoked R_p after MK-801 treatment shows little correlation between the two parameters (Figure 2.4A). However, comparing the initial R_p against the MK-801 induced change reveals that ROIs with the highest initial R_p see the largest decrease in R_p after treatment. These findings are consistent with the blockade of NMDA receptors during stimulation in MK-801 being due to evoked glutamate release alone, with little to no contribution from spontaneous neurotransmission. Taken together, these results indicate that the majority of synapses participate in both evoked and spontaneous neurotransmission while a small subpopulation (20%) may only receive spontaneous signals. The dynamics of NMDA receptor blockade with MK-801 illustrate that in synapses that receive glutamate from both modes of transmission, the NMDA receptors activated are largely unique to one mode or the other with limited overlap.

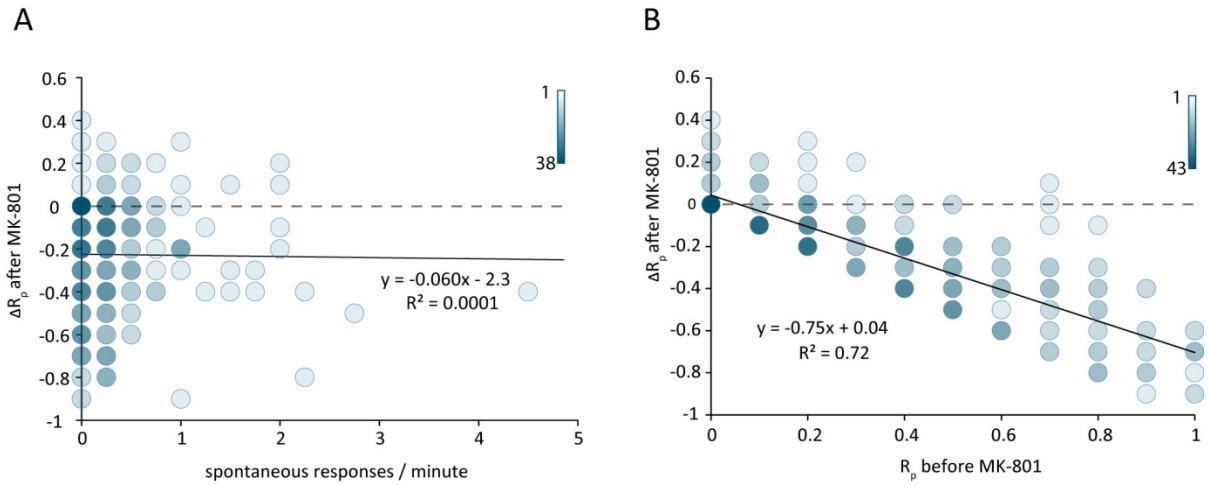

Figure 2.4 – Reduction in postsynaptic responses by MK-801 correlates with evoked response probability but not spontaneous response rate

A. Scatter plot of ΔR_p vs spontaneous response rate before MK-801 was added. For both plots N = 250 ROIs from 5 cells and 4 cultures. **B.** Scatter plot of the change in evoked response rate after MK-801 treatment (ΔR_p) vs initial evoked response rate. Shading indicates overlapping data points. Linear fit lines generated via least squares method.

Methods

Cell cultures : Prepared as described previously in (Reese and Kavalali 2015).

GCaMP6f-PSD95 Imaging : Tyrode's solution and equipment are the same as described previously. 8 hours after transfection, 40x images were collected at 5 frames per second with the lowest illumination possible and a neutral density 0.6 filter in the light path.

Event detection : 2.5 μm diameter circular ROI's were placed manually over puncta highlighted by subtracting the average of each pixel from its peak value in 10 second steps starting at the beginning of the experiment. In this way, 50 ROIs were selected per experiment in order of appearance. Fluorescence traces were obtained from each ROI and raw fluorescence values converted to a running $\Delta F/F_o$ using a 5 second baseline. A point was identified as a peak were identified if its $\Delta F/F_o$ was greater than 0.1, its slope calculated in 400 ms steps was greater than 687 units / sec and the peak value was greater than 2 standard deviations greater than the signal from the previous 2 seconds.

Statistics : All statistical tests were performed using Graphpad Prism 6.01.

CHAPTER THREE
Calcium Signaling in the Dendrite

CALCIUM SIGNALING DRIVEN BY THE ACTION POTENTIAL

Membrane depolarization drives Ca^{2+} influx through voltage-gated Ca^{2+} channels

By far the largest sources of Ca^{2+} flux across the plasma membrane into the dendrite are the voltage-gated Ca^{2+} channels (VGCCs). These channels are grouped broadly in to high voltage activated (HVA) subtypes L, N, P/Q and low voltage activated (LVA) subtypes R and T. In neocortical neurons, all of these channel subtypes are expressed in the initial portion of the dendrite, with the distal dendrites only expressing HVA channels (Magee, Christofi et al. 1995). Somatic VGCC currents are dominated by the L and N type channels (Fisher, Gray et al. 1990, Christie, Eliot et al. 1995).

HVA channels are opened in response to back-propagating action potentials (bAPs) as Na^{+} driven membrane voltage increases readily surpasses their activation voltages, generally around -10 to -20 mV (Plummer, Logothetis et al. 1989, Jaffe, Johnston et al. 1992). As well as being ubiquitous on the dendrite, HVA VGCCs have been shown to localize to dendritic spines, where they can contribute large Ca^{2+} signals that are confined to the spine head by the narrow neck of the spine in a manner regulated by their activity (Sabatini and Svoboda 2000, Bloodgood and Sabatini 2005). LVA channel types open in response to subthreshold voltage deflections, including those produced by unitary postsynaptic currents that fail to produce an action potential. T-type VGCCs in particular

have been shown to produce local Ca^{2+} influx in the dendrite in response to EPSP (Magee, Christofi et al. 1995). The activation curve of these channels is low enough that under resting conditions, channels may remain open and contribute significantly to the resting membrane potential (Magee, Avery et al. 1996).

Synaptic transmission drives postsynaptic Ca^{2+} influx

Excitatory synaptic transmission in the hippocampus involves the release of glutamate on to two primary types of postsynaptic receptors, the NMDA and AMPA receptors. AMPA receptors are relatively more numerous and under physiological conditions they pass the majority of the current that comprises the EPSP. AMPA receptors are ligand gated and nonselectively pass monovalent cations, which at low membrane voltages are largely Na^{+} ions. These receptors are made of four individual subunits and are expressed as heterotetramers with two pairs of matching subunits each i.e. a dimer of dimers. The subunits GluA1, GluA2, GluA3 and GluA4 are differentially expressed throughout the brain with the majority of receptors containing a dimer of GluA2 proteins (Borges and Dingledine 1998). Inclusion of the GluA2 subunit greatly decreases the single-channel conductance whilst preventing the channel from conducting Ca^{2+} ions and also conferring the inward rectification displayed by typical AMPARs (Swanson, Kamboj et al. 1997). However, receptors lacking the GluA2 subunits become Ca^{2+} permeable and contribute to the Ca^{2+} flux during of a synaptic EPSC (Washburn, Numberger et al. 1997). GluA2 is ubiquitously expressed throughout cortical structures, and with high expression levels in the hippocampus

making the majority of AMPA receptors Ca^{2+} impermeable (Vissavajjhala, Janssen et al. 1996). The critical role of GluA2-lacking AMPA receptors lies in their acute up-regulation after initiation of long-term potentiation (LTP) where they contribute to larger Ca^{2+} influxes in the potentiated synapses (Borges and Dingledine 1998, Guire, Oh et al. 2008).

NMDA receptors are also ubiquitous at the excitatory postsynapse as well as in the perisynaptic or extrasynaptic region. These receptors are gated by glutamate and are nonselective cation channels, exhibiting permeability to Na^{+}, K^{+} and Ca^{2+}. Mean open time is significantly longer than the AMPA receptor and studies dissecting NMDA contribution to mEPSCs show the NMDAR component to last upwards of 40ms (Espinosa and Kavalali 2009). Though the channel itself does not inherently exhibit voltage dependent current modulation, the external pore region is progressively blocked by Mg^{2+} ions at low voltages. The Mg^{2+} ion is driven by the electrochemical gradient but is too large to pass through the channel. This dynamic confers voltage dependent current flow through the NMDA receptor so that near resting voltage the current is minimal (Jahr and Stevens 1990).

The NMDA receptor is classically known as the Ca^{2+} source that drives the induction of LTP. The NMDAR is uniquely designed for this purpose as a coincidence detector of both pre and postsynaptic depolarization. The Mg^{2+} block of the channel pore is relieved during postsynaptic depolarization. If glutamate is coincident with this depolarization as is common during high frequency network activity, the resulting Ca^{2+} influx is considerably greater than during resting conditions which serves to drive Ca^{2+} dependent synaptic changes.

Glutamate release from the presynapse also activates metabotropic glutamate receptors (mGluRs). These receptors are not ion channels but rather propagate their signal

through the use of G-proteins. MGluRs fall into three categories based on their G protein association and cellular localization: Group 1 includes mGluR 1 and 5 which are coupled to the $G\alpha_q$ alpha subunit and are localized to the postsynaptic compartment, Group 2 (mGluR2 and 3) and Group 3 (mGluR 4, 6, 7 and 8) are predominantly localized to the presynaptic compartment and thus will not be discussed here (Shigemoto, Kinoshita et al. 1997). Upon glutamate binding to mGluR 1 or 5 the $G\alpha_q$ subunit is freed and activates phospholipase C (PLC). PLC cleaves lipids from the inner leaflet of the plasma membrane, separating the modified membrane lipid phosphatidylinositol 4,5-bisphosphate ($PIP_{2)}$ into a soluble group inositol 1,4,5-triphosphate (IP_3) and its insoluble membrane bound remainder 1,2-diacylglycerol (DAG). IP_3 signaling primarily functions to agonize IP_3 receptors on the endoplasmic reticulum (ER) while DAG functions to activate the Ca^{2+} dependent protein kinase (PKC) to phosphorylate its downstream targets.

CALCIUM SIGNALING DRIVEN BY INTERNAL STORES

The endoplasmic reticulum is a Ca^{2+} signaling organelle

Ca^{2+} signaling though various high-affinity receptors in the cytosol is made possible by the low resting concentration in neurons. In hippocampal cells, resting Ca^{2+} concentrations of around 130 nM (Elliott and Sapolsky 1993) are maintained by SERCA pumps moving Ca^{2+} into the endoplasmic reticulum (ER) and PMCA pumps moving Ca^{2+} into the extracellular space(Ebashi and Lipmann 1962, Van Amsterdam and Zaagsma 1986).

Efflux from the ER is the primary source of Ca^{2+} from within the cell and is regulated by, or interacts with many other cellular signaling motifs. There are two Ca^{2+} channels on the ER that facilitate this efflux, the ryanodine receptor (RyR) and the IP_3 receptor (Furuichi, Kohda et al. 1994).

The IP_3 receptor is gated by IP_3 and its coagonist ion, Ca^{2+}. At low nanomolar concentrations of Ca^{2+} the channel current is increased by Ca^{2+} with maximal activity near 200 nM. As the concentration rises, the channel becomes completely inhibited as cytosolic Ca^{2+} approaches 2 μM. This autoinhibitory mechanism produces bursting or oscillating behavior depending on the IP_3 concentration present (Wakui, Potter et al. 1989). The IP_3 receptor functions to integrate IP_3 and Ca^{2+} concentrations, providing a logic gate where IP_3 signaling only releases Ca^{2+} when the cytosolic concentration is low (Bezprozvanny, Watras et al. 1991).

The ryanodine receptor exists in 3 isoforms, 1, 2 and 3 which are homotetramers formed by 3 separately encoded genes (Orlova, Serysheva et al. 1996, Amador, Liu et al. 2009, Capes, Loaiza et al. 2011). All three isoforms are expressed in the hippocampus, with RyR2 and RyR3 predominating in other cortical regions (Giannini, Conti et al. 1995). These channels are unique in that they are gated by the ion that they pass, a mechanism called Ca^{2+}-induced-Ca^{2+} release (CICR). The Ca^{2+} dependent conductance takes a bell shaped curve, where high amounts of Ca^{2+} serve to close the channel (Bezprozvanny, Watras et al. 1991). RyR1 is opened by sub-micromolar concentrations of Ca^{2+} while RyR3 requires greater than 1 μM to open (Sonnleitner, Conti et al. 1998). While high (100 μM) concentrations of free Ca^{2+} are shown to inhibit the RyR, these conditions are rarely met as the channel inactivates

in roughly 6 ms (Schiefer, Meissner et al. 1995) producing transient Ca^{2+} concentrations around 5 μM in the dendrite (Larkum, Watanabe et al. 2003).

In addition to the Ca^{2+} ion itself, these channels are antagonized by various exogenous compounds such as ryanodine, the plant alkaloid for which the channel is named. However, there is only one known endogenous agonist, cyclic-ADP-ribose which is thought to play a regulatory role in preventing ER overfilling as well as signaling the ER to increase its CICR sensitivity activity (Verkhratsky and Shmigol 1996, Hashii, Minabe et al. 2000). This effect acts through the channel effector protein FKBP12 which functions to decrease channel sensitivity by stabilizing its closed state, especially for the RyR2 isoform (Meszaros, Bak et al. 1993, Brillantes, Ondrias et al. 1994, Ahern, Junankar et al. 1997). Phosphorylation of the channel by protein kinase A is also known to disrupt this RyR-FKBP interaction which produces an increase in receptor sensitivity (Marx, Reiken et al. 2000). The ubiquitous Ca^{2+} binding protein calmodulin (CaM) also binds to the RyR both in its Ca^{2+} bound and unbound states. CaM binding increases open probability at low Ca^{2+} concentrations and decreases it when Ca^{2+} is high which accounts for the channels bell shaped Ca^{2+} dependent conductance (Tripathy, Xu et al. 1995, Ikemoto, Takeshima et al. 1998).

The ER is host to Ca^{2+}-induced Ca^{2+} signaling

CICR is a Ca^{2+} signaling motif common to many cell types including pancreatic β cells, muscle cells and neurons. In neurons, CICR is known to be activated by both VGCC activity (Chavis, Fagni et al. 1996, Sandler and Barbara 1999) and by synaptic activity. This

is likely facilitated by the postsynaptic scaffolding protein homer, which forms functional Ca^{2+} signaling units by linking ER proteins with proteins on the plasma membrane. Homer is known to link group 1 mGluRs with IP_3 receptors and RyRs with the NMDAR via the adaptor protein shank (Tu, Xiao et al. 1998, Naisbitt, Kim et al. 1999, Tu, Xiao et al. 1999). Morphological studies corroborate these findings, as ER membrane has been shown to be present in dendritic spines very near to the postsynapse (Spacek and Harris 1997).

CICR may be initiated via several mechanisms which represent unique functions. Perhaps the best described is a positive feedback loop where IP_3 signaling opens the IP_3 receptor and the resulting calcium facilitates greater efflux by opening nearby RyRs (Bezprozvanny, Watras et al. 1991, Parker and Yao 1991, Miyakawa, Mizushima et al. 2001). In myocytes this motif is well described all along the sarcoplasm but in neurons IP_3 receptor clusters may form functional signaling domains near dendritic branches (Hertle and Yeckel 2007). Experiments in acute hippocampal slices indicate that CICR is also triggered directly by synaptic Ca^{2+} influx. NMDA Ca^{2+} transients in dendrites contain a component that is sensitive to ryanodine treatment, indicating that excitatory synaptic transmission is able to couple directly with ER Ca^{2+} stores (Emptage, Bliss et al. 1999, Kovalchuk, Eilers et al. 2000).

CHAPTER FOUR
Characterization of mEPSC driven Ca^{2+} transients in hippocampal neurons

ABSTRACT

Spontaneous glutamate release-driven NMDA receptor activity exerts a strong influence on synaptic homeostasis. However, the properties of Ca^{2+} signals that mediate this effect remain unclear. Here, using hippocampal neurons labeled with the fluorescent Ca^{2+} probes Fluo-4 or GCAMP5, we visualized action potential-independent Ca^{2+} transients in dendritic regions adjacent to fluorescently labeled presynaptic boutons in physiological levels of extracellular Mg^{2+}. These Ca^{2+} transients required NMDA receptor activity, and their propensity correlated with acute or genetically induced changes in spontaneous neurotransmitter release. In contrast, they were insensitive to blockers of AMPA receptors, L-type voltage-gated Ca^{2+} channels, or group I mGluRs. However, inhibition of Ca^{2+}-induced Ca^{2+} release suppressed these transients and elicited synaptic scaling, a process which required protein translation and eukaryotic elongation factor-2 kinase activity. These results support a critical role for Ca^{2+}-induced Ca^{2+} release in amplifying NMDA receptor-driven Ca^{2+} signals at rest for the maintenance of synaptic homeostasis.

INTRODUCTION

Studies in the last decade have shown that spontaneous release events trigger biochemical signaling leading to maturation and stability of synaptic networks, local dendritic protein synthesis and control postsynaptic responsiveness during homeostatic

synaptic plasticity (Chung and Kavalali 2006, Sutton, Ito et al. 2006, Kavalali 2014). Most surprisingly, these studies have demonstrated that postsynaptic excitatory receptor blockade or inhibition of neurotransmitter release in addition to action potential blockade induces faster and more pronounced homeostatic synaptic potentiation (Sutton, Ito et al. 2006, Nosyreva, Szabla et al. 2013). There is evidence that alterations in resting Ca^{2+} signaling, partly triggered via activation of NMDA receptors at rest, is critical for these effects (Wang, Zhang et al. 2011, Nosyreva, Szabla et al. 2013). However, to date there is no direct information on the properties of dendritic Ca^{2+} signals elicited by spontaneous release events under physiological circumstances. Our group's previous work as well as others used electrophysiology to show that, indeed, under physiological levels of extracellular Mg^{2+} spontaneous miniature excitatory postsynaptic currents (mEPSCs) possess a sizable NMDA receptor-mediated component, indicating that NMDA receptors signal at rest under physiological conditions without requiring local AMPAR-mediated dendritic depolarizations (Espinosa and Kavalali 2009, Povysheva and Johnson 2012, Gideons, Kavalali et al. 2014). The existence of an NMDA component within mEPSCs agrees with earlier estimates of incomplete Mg^{2+} block of canonical NMDA receptors near resting membrane potentials, and therefore it does not necessarily involve NMDA receptor subunits with altered Mg^{2+} sensitivity (Jahr and Stevens 1990). Nevertheless, the NMDA receptor Ca^{2+} influx under these conditions is estimated to be small, corresponding to approximately 20% of the full Ca^{2+} influx carried by unblocked NMDA receptors (Espinosa and Kavalali 2009). Therefore, as NMDA receptor-driven Ca^{2+} signals at rest are expected to be relatively minor in magnitude, it remains unclear how their blockade could be critical in producing homeostatic

synaptic scaling. To address this question, we visualized the resting NMDA receptor-driven Ca^{2+} signals and found that they are amplified by a Ca^{2+}-induced Ca^{2+} release mechanism to elicit downstream signaling events. Importantly, based on this information, we also show that direct suppression of these resting Ca^{2+} signals is sufficient to elicit eEF2 kinase dependent postsynaptic scaling.

RESULTS

Visualization of miniature spontaneous Ca^{2+} transients in hippocampal neurons

To detect transient Ca^{2+} signals that occur under resting conditions - in the absence of action potentials - we took advantage of the Ca^{2+} indicator dye Fluo-4 or the Ca^{2+} sensitive fluorescent protein GCaMP5K as reporters (Gee, Brown et al. 2000, Akerboom, Chen et al. 2012). To visualize synapses, both reporters were used on hippocampal neurons that were infected with lentivirus expressing the fusion protein Synaptobrevin2-mOrange (Syb2-mOrange) consisting of a chimera of the synaptic vesicle protein synaptobrevin2 with the pH sensitive red-shifted fluorophore mOrange (Ramirez, Khvotchev et al. 2012)(Figure 4.1A-D). In these experiments, the signal contribution of Syb2-mOrange during live imaging is negligible (see figure 4.2 supplement 1). In Fluo-4 experiments, neurons were initially incubated and labeled with the membrane permeable analog of Fluo-4 (Fluo-4 AM) (Figure 1A) followed by dye removal and perfusion with a Tyrode's solution containing 2 mM Ca^{2+}, 1.25 mM Mg^{2+} as well as 1 µM tetrodotoxin (TTX) to block action potentials. Fluorescence

images were collected at a frequency of 10 Hz and fluorescence intensity traces were generated for the regions of interest (ROIs) selected over Syb2-mOrange puncta which fluorescence was maximized at the end of each experiment using 50 mM NH_4Cl (Figure 4.1E). Under these conditions, we could detect rapid Ca^{2+} transients (miniature spontaneous calcium transients or mSCTs) with absolute values that were at least 2 standard deviations above the mean of the preceding baseline period (2 s) (Figure 4.1F). These events occurred at a frequency of 0.32 ± 0.04 min^{-1} per ROI, consistent with earlier estimates of the frequency of spontaneous fusion events per release site (Leitz and Kavalali 2014). Repeating the same experimental protocol with Fluo-4 AM in the absence of Mg^{2+} did not yield a significantly different mSCT frequency (Figure 4.1F) suggesting that under physiological Mg^{2+} concentrations we could detect a majority of mSCTs. Interestingly, even though the presence of extracellular Mg^{2+} is expected to greatly diminish NMDAR current magnitudes (Espinosa and Kavalali 2009, Gideons, Kavalali et al. 2014), imaging experiments did not reveal a significant difference in mSCT amplitudes detected in Mg^{2+} (1.25 mM Mg^{2+} $\Delta F/F_o = 0.063 \pm 0.001$, 0 mM Mg^{2+} $\Delta F/F_o = 0.067 \pm .002$, $p = 0.16$, Student's unpaired t-test, N = 825 events from 8 experiments). The fact that mSCT amplitude was unaffected by extracellular Mg^{2+} indicates mSCTs measured by Fluo-4 AM were not likely to be solely dependent on NMDA receptor activity.

In parallel experiments, we delivered the salt form of Fluo-4 (200 μM) with a patch pipette in the whole-cell recording configuration and performed the same imaging protocol as above (Figure 4.1B). In this setting, we detected a lower frequency of events (0.125 ± 0.035 min^{-1} per ROI), indicating that some of the mSCTs may be susceptible to postsynaptic

dialysis and wash out of soluble factors (Figure 4.1F). In agreement with this premise, when the same optical recording conditions were applied to neurons expressing a soluble version of the green emission Ca^{2+} indicator probe GCaMP5K, we could detect a higher frequency of mSCTs (0.230 ± 0.04 min^{-1} per ROI).

In subsequent experiments, we expressed a fusion construct of GCaMP5K with the postsynaptic scaffolding protein PSD95 (GCAMP5K-PSD95) in order to target the calcium sensor specifically to the postsynaptic density (Figure 4.1D). In the presence of extracellular Mg^{2+} based on the population average this setting provided the lowest estimate for the mSCT frequency (0.009 ± 0.004 min^{-1} per ROI) (Figure 4.1F). In contrast, removal of Mg^{2+} augmented the mSCT detection rate to a level comparable to the rates we observed with Fluo-4 or soluble GCaMP5K (Figure 4.1E). This finding suggests that, in the presence of Mg^{2+}, postsynaptically localized GCaMP5K-PSD95 has limited ability to detect the Ca^{2+} signals generated in its vicinity via Ca^{2+} influx. However, experiments in the absence of Mg^{2+} indicate that this probe is functional and can in principle detect these spontaneous local Ca^{2+} transients as reported earlier (Leitz and Kavalali 2014).

Recording in the presence of 1.25 mM Mg^{2+} and 1 μM TTX, we could detect spontaneously generated Ca^{2+} transients in the dendrites of hippocampal pyramidal cells with all four techniques. Although, each probe reports a different frequency these differences are statistically insignificant except when considering the difference between Fluo-4 AM and GCaMP5K-PSD95 (Figure 4.1F). Relatively lower detection efficiency of GCAMP5K-PSD95 compared to soluble probes illustrates that the majority of these transients are not localized to the postsynaptic density. The failure of Mg^{2+} to decrease mSCT amplitudes as

measured with Fluo-4 AM strongly suggest that a majority of transients are generated by a signaling process downstream of Ca^{2+} entry rather than reporting the Ca^{2+} influx per se. In order to identify the nature of this signaling, in subsequent experiments, we used the Fluo-4 AM based imaging to test conditions that alter mSCTs.

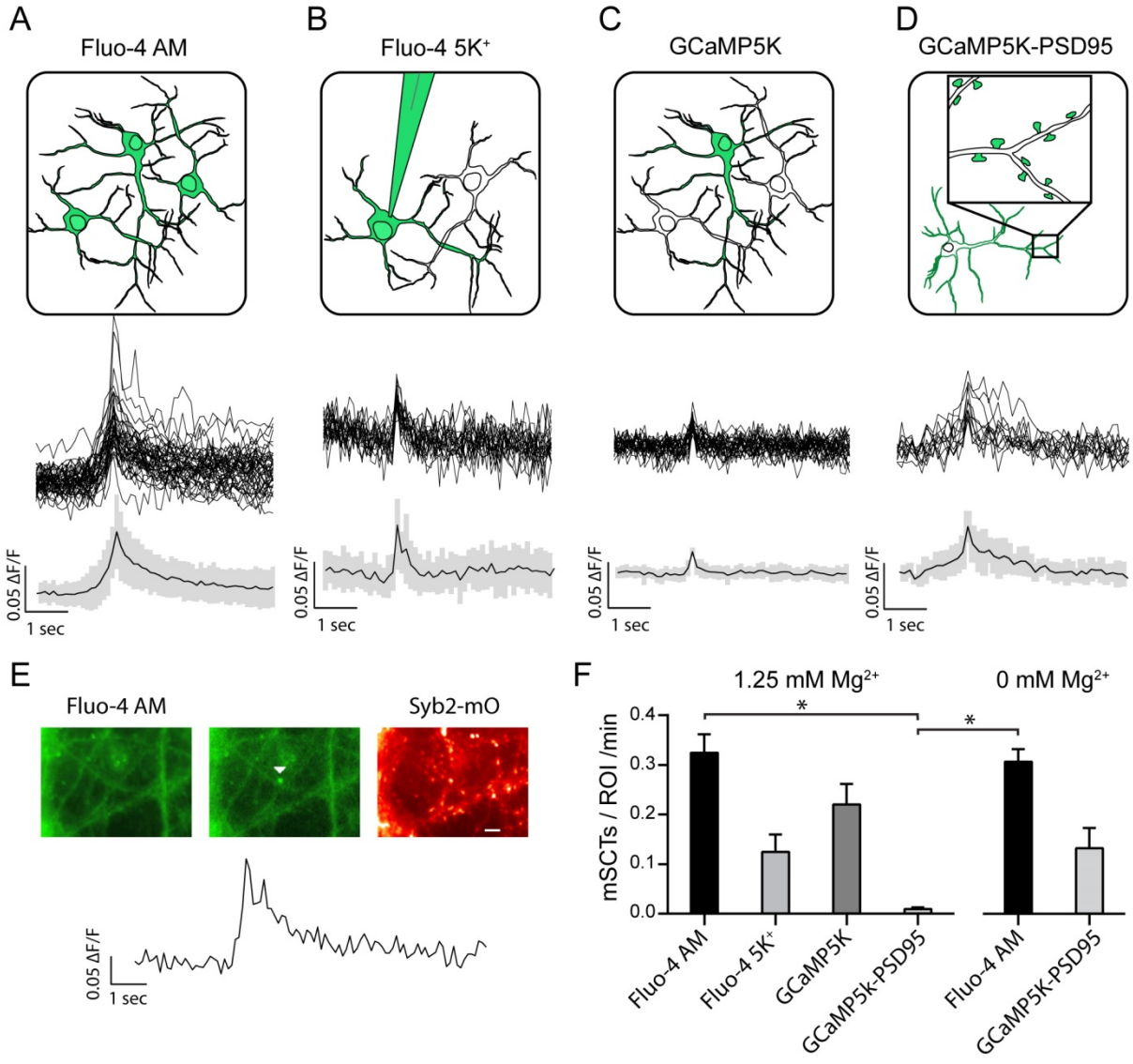

Figure 4.1 - Multiple approaches to detect miniature spontaneous Ca^{2+} transients (mSCTs) in the presence of TTX and physiological Mg^{2+}.

A. Loading dissociated rat hippocampal cultures with Fluo-4 AM dye labels all cells on the coverslip (above) and produces the largest signal amplitudes, shown as example traces and an average with standard deviation (below) N = 38 experiments, 7 cultures. B. Individual neurons were loaded with the salt form of Fluo-4 at the whole cell recording configuration via a pipette containing 200 μM of the dye. N = 4 experiments, 1 culture. C. Low efficiency lipotransfection with the highly sensitive GCaMP5K variant produces sparse labeling of neurons across the coverslip but low signal (ΔF/F) amplitudes. N = 5 experiments, 1 culture D. Lentiviral mediated transfection with GCaMP5K-PSD95 targets the fluorescent construct to the postsynaptic densities of all cells on each coverslip. N = 15 experiments, 4 cultures. E. Example images and trace of a mSCT visualized with Fuo-4 AM and its corresponding Syb2-mOrange puncta. Panels show baseline and peak fluorescence intensity with the arrow marking peak fluorescence intensity of the mSCT. Scale bar 5 μm. F. Frequencies expressed as mSCTs per ROI per minute show the highest efficiency of mSCT detection with Fluo-4 AM. Fluo-4 AM based experiments performed with no Mg^{2+} in the external solution reported no significant changes in mSCT compared to the presence Mg^{2+}. The postsynaptically localized reporter GCaMP5K-PSD95 reports statistically lower frequencies when compared to Fluo-4 AM (Fluo-4 AM 1.25 mM Mg^{2+} vs. GCaMP5K-PSD95 1.25 mM Mg^{2+} $p = 0.0003$, Fluo-4 AM 0 mM Mg^{2+} vs. GCaMP5K-PSD95 1.25 mM Mg^{2+} $p = 0.0031$, via one-way ANOVA with Holm-Sidak's multiple comparisons) 0 mM Mg^{2+} Fluo-4 AM N = 16 experiments, 8 cultures. 0 mM Mg^{2+} GCaMP5kK-PSD95 N = 10 experiments, 4 cultures.

The generation of mSCTs requires NMDA receptor mediated Ca^{2+} influx

To characterize mSCTs, neurons were labeled with Fluo-4 AM as in Figure 4.1A and imaged in Tyrode's solution containing TTX (Figure 4.2A). Ca^{2+} transients were detected by the slope of the rising phase as well as the peak amplitude. To ensure that these detected

peaks were not noise, only mSCTs with a peak amplitude 2 standard deviations greater than the signal average of the previous two seconds were counted. Figure 4.2B shows the rise and decay times as well as the fluorescence amplitudes of 306 mSCTs identified from 6 experiments. In these experiments, the mean rise time was 0.38 s with a median of 0.29 s. The mean decay time was 0.86 s with a median of 0.47 s. The amplitude distribution had an average $\Delta F/F_o$ of 0.061 with a median of 0.049 (Figure 4.2B).

Next we tested whether NMDA receptor activity is required for the generation of mSCTs. For this purpose, synaptic ROIs were imaged in three steps. First optical recordings were obtained in Tyrode's solution with nominal Ca^{2+} containing 1 μM TTX followed by the addition of 2 mM Ca^{2+} and finally in Tyrode's solution containing TTX + 2 mM Ca^{2+} + 50 μM AP5 (Figure 4.2C). In the absence of Ca^{2+} in the bath, mSCTs were virtually undetectable suggesting that Ca^{2+} influx is required for their generation. Switching the Tyrode's solution to TTX + 2 mM Ca^{2+} brought the mSCT frequency back to normal levels, and subsequent addition of the NMDA receptor antagonist AP5 again decreased the mSCT frequency to very low levels that were not statistically different from the nominal Ca^{2+} condition (Figure 4.2D). These results indicate that Ca^{2+} influx through the NMDA receptor is critical for the generation of mSCTs.

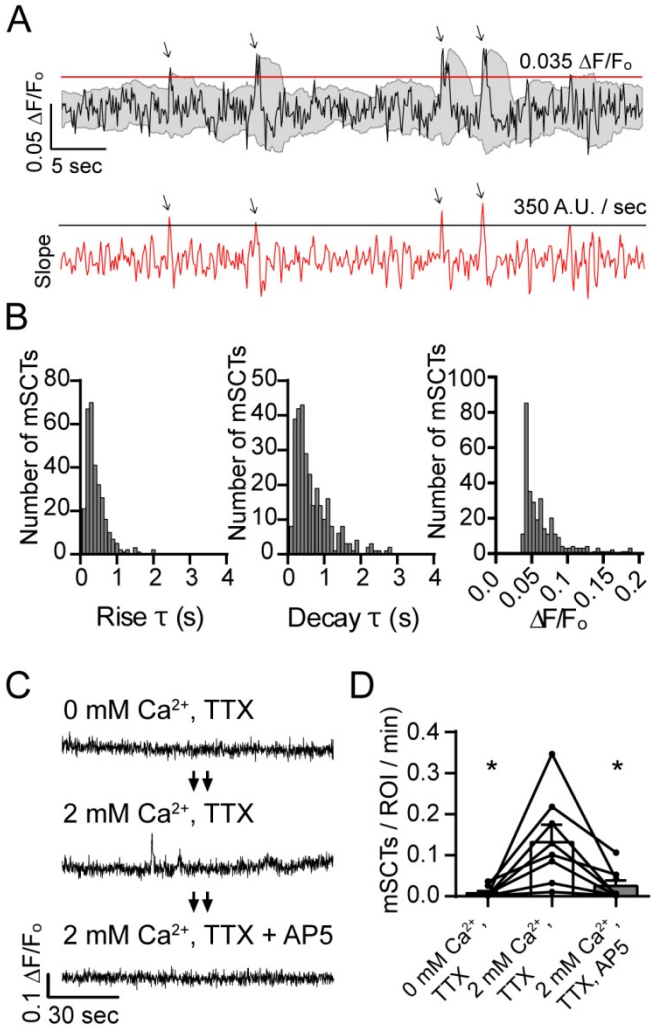

Figure 4.2 - Detection and characterization of spontaneous Ca^{2+} transients in physiological concentrations of Mg^{2+}.

A. Events detected from Fluo-4 AM traces having rising slope greater than 350 fluorescence units/sec and a peak $\Delta F/F_o$ greater than 0.035 were counted if the peak fluorescence value was 2 standard deviations greater than the mean of the signal 2 seconds previous. Gray shaded region indicates the moving average plus/minus two standard deviations and the red line indicates the 0.035 $\Delta F/F_o$ threshold. Red trace shows the 2 point slope with the black line as the 350 A.U. / second detection threshold. Arrows indicate peaks that satisfy these criteria. B. Histograms showing rise time (τ), decay time (τ) and amplitudes ($\Delta F/F_o$) of mSCTs. N = 306 mSCTs from 6 experiments and 2 cultures. C. Traces from cells (left) and Ca^{2+} transient frequencies (right) were obtained by imaging first in Tyrode's solution containing no Ca^{2+}, then in Tyrode's containing 2 mM Ca^{2+} and finally Tyrode's containing 2mM Ca^{2+} and the NMDA receptor blocker AP5. Removal of extracellular Ca^{2+} or block of the NMDA receptor resulted in a significant reduction in Ca^{2+} transient frequency (2 mM Ca^{2+} vs 0 mM Ca^{2+} P=0.038, 2 mM Ca^{2+} vs 2 mM Ca^{2+} + AP5 p = 0.038, via 1-way ANOVA with Holm-Sidak's multiple comparisons test). N=8 experiments, 2 cultures.

mSCTs are driven by spontaneous neurotransmitter release

To examine whether the NMDA receptor openings driving mSCTs were due to spontaneous glutamate release we took two complementary approaches. First, we took advantage of the fact that the acute application of 100 mM hypertonic sucrose is known to produce an increase in mEPSCs (Fatt and Katz 1952, Rosenmund and Stevens 1996). To measure this effect, hippocampal pyramidal cells were voltage clamped at -70 mV while a baseline AMPA mEPSC frequency was collected in Tyrode's solution containing 1 μM TTX, 50 μM PTX and 50 μM AP5 for 2 minutes. Perfusion was then switched to Tyrode's containing 100 mM hypertonic sucrose as the recording continued for 2 minutes. Quantification of these recordings revealed a 2.6-fold increase in mEPSC frequency upon the addition of hypertonic sucrose (Figure 4.3A). To test whether the increase in mEPSC frequency could drive an increase in mSCT frequency the experiment was repeated in neurons loaded with Fluo-4 AM. The baseline was collected in Tyrode's solution containing only TTX before changing to a solution containing TTX + 100 mM sucrose. The addition of hypertonic sucrose produced a 2.3 fold increase in mSCT frequency (Figure 4.3B), which supports the hypothesis that spontaneous glutamate release can drive the generation of postsynaptic calcium transients.

Next, to assess whether a decrease in mEPSC frequency would correlate with a decrease in mSCT frequency, we utilized neurons from mice lacking the critical SNARE-mediated fusion machinery component SNAP-25 (Washbourne, Thompson et al. 2002). These mice die at birth; however, hippocampal neurons cultured from embryonic mice form

synapses and manifest a virtual absence of evoked neurotransmission and highly diminished rate of spontaneous neurotransmitter release (Bronk, Deak et al. 2007). In Fluo-4 AM imaging experiments with hippocampal cultures made from littermate control mice, the application of AP5 was able to produce a significant decrease in mSCT frequency compared to baseline recorded in TTX, as had been observed previously in wild-type rat cultures. Neurons derived from SNAP25 knock out animals had a significantly decreased baseline mSCT frequency. Also, these transients remained sensitive to AP5, which is again consistent with mSCT generation being driven by spontaneous vesicle release (Figure 4.3C, D).

Figure 4.3 – mSCT frequency is correlated with mEPSC frequency.

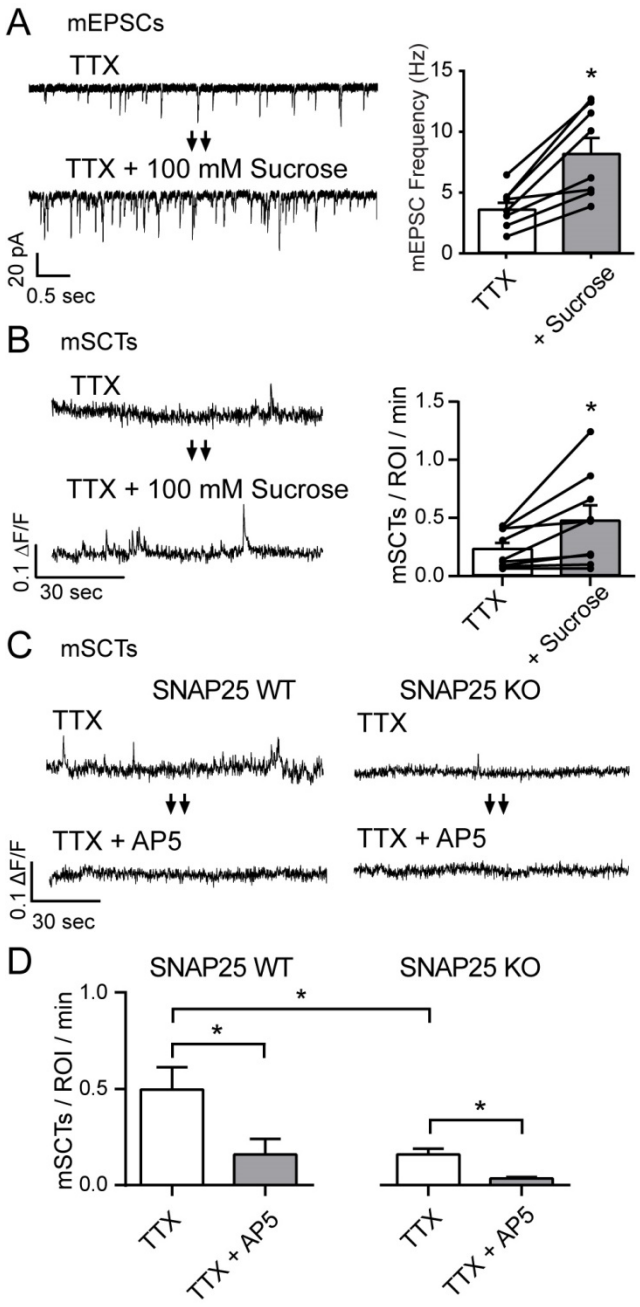

A. Whole cell recordings from WT cells (left) show a ~2 fold increase in mEPSC frequency when switched to Tyrode's solution containing 100 mM sucrose (right) ($p = 0.002$, Student's paired T test, N=8 cells, from 5 coverslips and 2 cultures). B. Example traces (left) and quantification of spontaneous Ca^{2+} transient frequencies measured via imaging show a ~2 fold increase upon application of 100 mM sucrose (right) ($p = 0.028$, Student's paired T test, N=9 experiments from 3 cultures). C. Fluo-4 example traces from both control and SNAP25 KO animals before and after the application of AP5. D. Fluo-4 imaging in cultures made from SNAP25 KO and littermate control mice reveal that the KO cultures have a substantially decreased mSCT frequency. In this setting, AP5 treatment greatly decreases but does not completely abolish the remaining mSCTs. (WT, TTX vs WT, TTX+AP5 $p = 0.010$. WT, TTX vs KO, TTX $p = 0.008$. KO TTX vs KO TTX+AP5 $p = 0.003$, via 1-way ANOVA with Tukey's multiple comparisons, N=8 experiments in WT cells and 9 experiments in KO cells from 3 cultures).

mSCTs do not require activation of AMPA receptors, L-type Ca^{2+} channels, or group I mGluRs

Mature glutamatergic synapses contain both AMPA and NMDA receptors (Bekkers and Stevens 1989, Liao, Scannevin et al. 2001). Therefore, in the next set of experiments we tested whether concurrent AMPA receptor activity augments NMDA receptor activity at rest through electrical means. Such synergy between the activation of the two types of receptors may be facilitated by dendritic spines that possess a high spine neck resistance that render them electrically isolated from the dendritic shaft (Bloodgood and Sabatini 2005, Harnett, Makara et al. 2012) but see (Popovic, Gao et al. 2014). In this way activation of AMPA receptors may result in sufficient local depolarization to facilitate relief of adjacent NMDA receptors from Mg^{2+} block. Additionally, AMPA receptors lacking GluA2, which are calcium-permeable, could also contribute to these transients (Hollmann, Hartley et al. 1991). To examine the role of AMPA receptor activation on mSCTs, we performed the same analysis above in the presence of AMPA receptor antagonist 2,3-dihydroxy-6-nitro-7-sulfamoyl-benzo[f]quinoxaline-2,3-dione (NBQX). In these experiments NBQX (5μM) did not affect mSCT frequency (Figure 4.4A). This argues against a direct (e.g via calcium-permeable GluA2 lacking receptors) or indirect (via local depolarization) contribution of AMPA receptors to mSCTs (Figure 4.4A).

Although experiments presented above showed that the NMDA receptor activity is responsible for triggering the majority of mSCTs in response to spontaneous glutamate

release, it remains possible that L-type Ca^{2+} channels may also contribute this activity as they have been shown to open near resting membrane potentials (Kavalali and Plummer 1996, Magee, Avery et al. 1996). Therefore, we also tested if L-type Ca^{2+} channel activity contributed to the mSCT activity. In these experiments, treatment with the L-type Ca^{2+} blocker nimodipine (5μM) did not significantly affect mSCT frequency (Figure 4.4B) indicating that these channels do not contribute to the Ca^{2+} transients. However, here we should note that L-type channel activity may still be involved in setting resting Ca^{2+} levels and thus impact signaling (Wang, Zhang et al. 2011). Despite producing no change in mSCT frequency in this assay, nimodipine was able to decrease Ca^{2+} influx in a separate assay (figure 4.4 supplement 1).

In subsequent experiments we also tested the potential role of G_q-coupled metabotropic glutamate receptor subtypes 1 and 5 in maintenance of Ca^{2+} transients. These group I mGluRs can affect Ca^{2+} signaling via activation of phospholipase C and IP3 generation (Skeberdis, Lan et al. 2001, Topolnik, Azzi et al. 2006). However, application of the mGluR1 antagonist YM202074 and mGluR5 antagonist Fenobam did not cause a significant change in mSCT frequency, indicating that activation of these receptors does not contribute to these Ca^{2+} transients (Figure 4.4C). Despite producing no change in the measured mSCT frequency, these drugs were shown to be blocking their target receptors in a separate assay (figure 4.4 supplement 2).

mSCT generation requires Ca^{2+} release from internal stores

In hippocampal pyramidal cells, NMDA receptor opening by evoked glutamate release elicits larger Ca^{2+} transients through a Ca^{2+}-induced Ca^{2+} release mechanism (Lei, Zhang et al. 1992, Emptage, Bliss et al. 1999). In this form of signaling, the small Ca^{2+} transient produced by the NMDA receptor opening raises internal Ca^{2+} concentrations near ryanodine receptors (RyRs) on the endoplasmic reticulum high enough to cause their opening at which point a much larger transient is generated. To test whether this mechanism plays a role in the mSCTs we observe, we imaged with Fluo-4 AM in the presence of dantrolene, which is known to reduce the Ca^{2+} sensitivity of RyR1 and 3 by blocking their interaction with calmodulin (Fruen, Mickelson et al. 1997). Indeed, when compared to the TTX baseline, cells imaged with TTX + dantrolene had a significantly reduced mSCT frequency (Figure 4D). This finding was validated by using ryanodine, which directly blocks all three RyR isoforms in a use-dependent manner (Hawkes, Nelson et al. 1992, Meissner and el-Hashem 1992). To facilitate use-dependent block of RyRs by ryanodine, the baseline mSCT frequency was first collected in TTX and then cells were perfused for 13 minutes with a solution containing 30 μM ryanodine without TTX to maximize RyR opening and ryanodine block. The cells were then perfused with Tyrode's containing TTX + ryanodine for 2 minutes before continuing the recording. Under these conditions, the application of ryanodine produced a ~5-fold decrease in mSCT frequency (Figure 4.4E). In addition, the Ca^{2+} transients that were detectable after ryanodine treatment were substantially decreased in

amplitude suggesting that they are likely to be produced by a subpopulation of RyRs that remained unblocked or incompletely blocked (average TTX $\Delta F/F_o = 0.052 \pm 0.001$, TTX + Ryanodine $\Delta F/F_o = 0.045 \pm 0.001$, $p = 0.002$ Student's unpaired t-test, n = 199 events in TTX, 110 events in TTX + ryanodine, 8 experiments, 2 cultures). Treatment with dantrolene or ryanodine is presumed to decrease mSCT frequency by blocking RyRs responsible for producing the Ca^{2+} transient. With these inhibitors present, further NMDA openings can no longer trigger an mSCT. In fact, the efficacy of ryanodine in this case allowed further investigation of the pure NMDA transient under these experimental conditions. We incubated neurons with ryanodine for 15 minutes to block RyRs and then loaded them with Fluo-4 AM as before. These cells were imaged in Tyrode's solution containing TTX but no extracellular Mg^{2+} to allow maximal NMDA currents. Under these conditions Ca^{2+} transients were observed, but when 1.25 mM Mg^{2+} was again added no further transients could be measured (Figure 4.4F). These results illustrate that under physiological concentrations of Mg^{2+}, Fluo-4 cannot detect the NMDA Ca^{2+} transient without further amplification from Ca^{2+} induced Ca^{2+} release.

Figure 4.4 - Spontaneous Ca^{2+} transient generation is decreased by blocking release of Ca^{2+} release from internal stores but not by blocking the AMPA receptors, L-type Ca^{2+} channels or group I mGluRs.

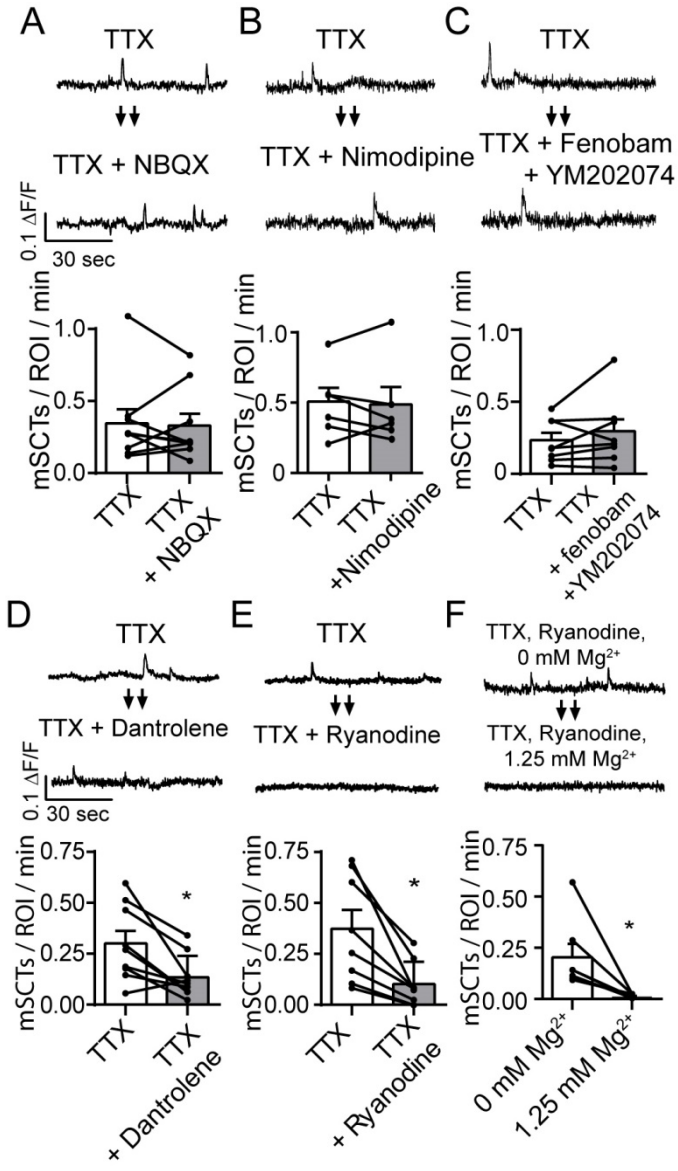

A. Traces (top) from images taken before and after treatment with the AMPA receptor blocker NBQX show no change in Ca^{2+} transient frequency (bottom) ($p = 0.78$ with Student's paired t-test, N = 9 experiments, 2 cultures). B. Imaging in the presence of the specific L-type calcium channel blocker nimodipine (5μM) does not affect spontaneous Ca^{2+} transient frequency (bottom) ($p = 0.89$ with Student's paired t-test. N = 7 experiments 1 culture). C. Imaging in the presence of mGluR1 and mGluR5 blockers YM202074 and fenobam produce no differences in spontaneous Ca^{2+} transient frequency ($p = 0.26$ via Student's t-test. N = 8 cells, 2 cultures). D. Application of internal Ca^{2+} store blocker dantrolene produces a significant drop in mSCT frequency in before/after experiments. ($p = 0.008$, Student's paired t-test, N = 9 experiments, 3 cultures). E. Fluo-4 AM example traces and frequency quantification from cells recorded in TTX then in TTX + 30 μM Ryanodine. In before/after imaging experiments, 15 minute treatment of the use dependent ER Ca^{2+} channel blocker ryanodine decreased the frequency of observed Ca^{2+} transients ($p = 0.004$, N = 8 via Student's paired t-

test). F. Example traces and frequency quantification of cells pre-treated with ryanodine and then imaged first in Tyrode's solution containing no Mg^{2+} followed by Tyrode's solution containing 1.25 mM Mg^{2+}. Ca^{2+} transients are measured in Mg^{2+} free solution but not in 1.25 mM Mg^{2+}. ($p = 0.024$, via Student's unpaired t-test. N = 7 experiments 2 cultures.)

DISCUSSION

In this study, we took advantage of multiple Ca^{2+} indicator probes to examine the properties of Ca^{2+} transients detected in hippocampal neurons in physiological levels of extracellular Mg^{2+} in the absence of action potentials. These transients are important because they are key to understanding the Ca^{2+} signaling events occurring at rest that result in regulation of protein translation and gene transcription leading to synaptic plasticity (Chen, Wang et al. 2014, Lalonde, Saia et al. 2014) (for review see Kavalali, 2015). Under these conditions we detected robust NMDA receptor dependent Ca^{2+} transients at a rate of 0.32 ± 0.03 min^{-1} where previously our group was able to measure a per synapse spontaneous release rate of 0.76 ± 0.03 min^{-1} by imaging with presynaptic probes (Leitz and Kavalali 2014). The relatively higher release rate measured earlier may suggest that not every release event is able to generate an mSCT. The link between these Ca^{2+} transients and spontaneous neurotransmitter release was verified by the parallel increase in mSCT and spontaneous neurotransmitter release frequencies in response to application of hypertonic sucrose. Furthermore, the frequency of Ca^{2+} transients was also significantly diminished in neurons lacking SNAP-25, which show a substantial reduction in spontaneous release, and in cultures treated with NMDA receptor blockers.

Interestingly GCaMP5K-PSD95, a probe located near the postsynaptic density, revealed only a very small number of events that fulfilled our detection criteria while soluble probes proved to be much better indicators. This observation indicates that although mSCT generation depends on NMDA receptor driven Ca^{2+} influx, this does not result in strong signals at the postsynaptic density. Rather, mSCTs seem to rely on the activation of Ca^{2+} release from smooth endoplasmic reticulum which is present in spines or adjacent dendritic regions (Spacek and Harris 1997).

The generation of mSCTs was not dependent on AMPA receptors, L-type Ca^{2+} channels or postsynaptic metabotropic glutamate receptor subtypes 1 and 5. While all of these play a role in Ca^{2+} dynamics under other circumstances the mSCTs we observed under resting conditions were primarily driven by the coupling of the NMDA receptor to internal Ca^{2+} stores through the ryanodine receptor, as the application of dantrolene or ryanodine produced a marked reduction in both mSCT frequency and amplitude. Earlier studies performed in hippocampal synapses discovered that unitary evoked EPSCs were accompanied by Ca^{2+} transients that were only minimally dependent on voltage gated Ca^{2+} channels or AMPA receptors. However, unlike the mSCTs we observe, the application of ryanodine produced only a small reduction in Ca^{2+} transient amplitude in these experiments (Kovalchuk, Eilers et al. 2000). This difference may suggest that spontaneous glutamate release-driven Ca^{2+} transients are more dependent on internal Ca^{2+} stores compared to Ca^{2+} transients elicited by evoked release.

Methods

Cell Culture

Hippocampal cultures from Sprague-Dawley rats or eEF2 kinase knockout mice and their wild-type littermate controls were generated from postnatal day 1-3 male and female pups and plated on Matrigel (Corning Inc, NY) coated coverslips as described previously (Kavalali, Klingauf et al. 1999). Neurons were infected with lentivirus at 4 days *in vitro*. Neurons were used for experiments between 14 to 18 days *in vitro*.

Dissociated hippocampal cultures from SNAP25 knockout mice and their wild-type littermates were generated from E17-20 embryos and were plated on poly-d-lysine coated coverslips as described previously (Bronk, Deak et al. 2007). Neurons were used for experiments 14-18 days *in vitro*.

Ca^{2+} Imaging

Fluo-4 AM imaging: Neurons were incubated for 10 minutes in culture media containing 5.6 μM Fluo-4 AM (Life Technologies, Grand Island NY). Coverslips were then removed and washed for 2 minutes prior to recording with Tyrode's solution containing (in mM) 150 NaCl, 4 KCl, 1.25 $MgCl_2$, 2 $CaCl_2$ and 10 TES buffer, pH adjusted to 7.4. Where solutions are noted to have 0 mM Ca^+ the solution is prepared from deionized water with no added Ca^{2+}. All solution changes except +100 mM hypertonic sucrose include 2 minutes of wash time in the new solution to ensure full application of the new conditions. Neurons were

imaged using a 40x objective on a Nikon TE2000-U microscope. Images were collected at 10 frames per second using an Andor xION Ultra EMCCD camera for a duration of ~ 2 minutes. Event frequencies per ROI were estimated using the population average obtained from 72 ROIs monitored per experiment. Our analysis, therefore, refers only to average per ROI frequency per experiment. Illumination was provided by a Sutter DG-4 arc lamp using a 470±40 nm bandpass excitation filter. Post experiment synapse visualization used a 548±10 nm filter to excite Syb2-mO and Tyrode's solution containing 50 mM NH_4Cl to maximize fluorescence. The emission filter in place allowed 515 ± 15 nm and 590 ± 20 nm bands to pass. Fluo-4 traces were generated by measuring circular regions of interest (ROI), 3 μm radius centered over Syb2-mO puncta.

Single cell Fluo-4 imaging: Uninfected neurons were loaded with indicator by using the whole cell voltage clamp configuration described above. The patch pipette contained 200 μM Fluo-4 pentapotassium salt (Life Technologies, Grand Island NY).

Soluble GCaMP5K imaging: Wild type neurons expressing Syb2-mO were transfected with pFU-GCaMP5K using lipofectamine 3000 (Life Technologies, Grand Island NY) 8 hours prior to imaging. Images were collected as above.

GCaMP5K-PSD95 imaging: Neurons expressing GCaMP5K-PSD95 via lentiviral infection were imaged as indicated above except using a 100x objective. Images were collected at 8 frames per second to minimize single frame noise.

Ca^{2+} transient analysis and statistics: Ca^{2+} transient frequency was derived from imaging traces by counting Ca^{2+} transients where the signal peak had a 2-point slope greater than 70 A.U. (350 units/sec over a 200 ms window) and amplitude greater than 0.035 $\Delta F/F_o$. Ca^{2+} signals were not counted if their peak width was greater than 5 seconds. Maximum peak amplitude was required to be 2 standard deviations greater than the mean of the signal in the previous two seconds. Single high points were not counted. Detected peaks were ignored if another peak was detected in the following 400ms to prevent the double counting of slower mSCTs. All error bars represent standard error of the mean except in Figure 1A-D where standard deviation is used. Rise and decay times are displayed as τ, where τ is the time in seconds necessary to reach $\left(1-\frac{1}{e}\right)\Delta F$ for the rising phase or $\left(\frac{1}{e}\right)\Delta F$ for the decay phase based on a single exponential fit line obtained with Axon Clampfit 9.0.1.07. All statistical tests were performed using Graphpad Prism 6.01.

CHAPTER FIVE
Homeostatic Synaptic Plasticity Modifies the Strength of Neuronal Input

Multiplicative scaling of the synapse

In 1949, even before the first description of minis, it was observed that denervated skeletal muscle became hypersensitive to neurotransmitter (Cannon, Rosenblueth 1949). Further study of this effect led to the discovery that the induction of hypersensitivity occurs before the axon withdraws and is thus related to activity deprivation rather than axon contact (Colman, Nabekura et al. 1997). These were the first observations of the ability of synapses to scale their strength in response to input activity or the lack thereof. In central synapses, the critical first study of this phenomenon was done by Dr. Gina Turrigiano in 1998 where she was able to show that in neocortical cultures, blocking action potentials or AMPA EPSCs led to an increase in quantal response amplitudes while suppressing GABA currents, which serves to increase culture activity, led to a decrease in quantal response amplitudes (Turrigiano, Leslie et al. 1998). In experiments where exogenous glutamate was applied, the authors showed that these changes were largely due to an increase in postsynaptic strength rather than a presynaptic change. It was also noted in this publication that the shift in quantal response strength, measured as mEPSC amplitude, changed in a multiplicative fashion and all synapses were changed by the same percent. This fact would mean that after synaptic scaling, the relative synaptic weights across the cell would be preserved. The authors described the exciting possibility that this compensatory synaptic scaling may stabilize the cells output firing during

development, or even provide a way to normalize its synaptic inputs after multiple LTP or LTD events.

Minis control synaptic scaling

Further studies went on to demonstrate that activity-dependent scaling involved the insertion of AMPA receptors into the postsynapse and that these receptors were newly synthesized rather than pre-existing (Ju, Morishita et al. 2004). Around the same time, a different group led by Dr. Erin Schumann demonstrated that protein synthesis in the dendrites was controlled by minis (Sutton, Wall et al. 2004). In these experiments, the authors showed if action potentials and mEPSCs were suppressed, the expression of a reporter was greatly increased compared to only suppressing action potentials. This study was critical, as it implicated miniature release in regulating postsynaptic parameters.

The direct link illustrating that minis can control synaptic strength was published by the same group in 2007. This study, showed definitively that blocking mEPSCs induced synaptic scaling not only to a greater extent, but also much faster than only blocking action potentials (Sutton, Ito et al. 2006). Synaptic scaling in this study was again proven to be protein synthesis dependent, but the mechanism was not described. A year later, new experiments showed that the mEPSC blockade drives an increase in dendritic protein synthesis is accompanied by a dramatic shift in the phosphorylation state of eEF2 (Sutton, Taylor et al. 2007). eEF2 is a eukaryotic elongation factor that is necessary for ribosomal function. When eEF2 is dephosphorylated it is free to participate

in the elongation of mRNA transcripts in the ribosome, but in the absence of action potentials, minis suppress protein synthesis by promotes the phosphorylated, deactivated states of eEF2. The key detail in this investigation was the finding that the NMDAR was required for this effect. In a separated well culture system, it was shown that application of the NMDAR blocker AP5 only to the postsynaptic side of the culture was sufficient to turn on protein synthesis in the dendrites.

Involvement of the NMDAR in controlling protein synthesis dependent synaptic scaling would imply that the critical signal is Ca^{2+} driven. This hypothesis was supported by the fact that the kinase known to phosphorylate eEF2, CaMKIII also known as eEF2 kinase has a very high affinity for CaM and thus would be stimulated by very low amounts of Ca^{2+} (Hughes, Smith et al. 1993). Further evidence for the Ca^{2+} mediated hypothesis came from the group of Dr. Lu Chen in 2011 where they showed that in their model system, chelating internal Ca^{2+} could induce synaptic scaling.

This study however proposed a different mechanism. In cultured neurons, blocking action potentials and the NMDAR was shown to induce the synthesis of retinoic acid. Surprisingly, the acute application of retinoic acid was sufficient to induce synaptic scaling in cultured neurons, and to induce protein synthesis of AMPAR subunits in a synaptosome model. Further experimentation showed that retinoic acid was also necessary, as blocking is induction prevented synaptic scaling (Aoto, Nam et al. 2008). In this model, retinoic acid is responsible for affecting local dendritic protein synthesis through the dendritically localized retinoic acid receptor RARα (Maghsoodi, Poon et al. 2008). It is yet unclear how low Ca^{2+} concentrations might induce retinoic acid synthesis

or how RARα activity might function to stimulate protein synthesis. Further work is needed, as it is currently unknown if the eEF2K mediated pathway and the retinoic acid pathway represent part of the same mechanism or perhaps divergent regulatory mechanisms.

CHAPTER SIX
Experimental Evidence for the Induction of Synaptic Scaling Through mEPSC Driven Ca^{2+} Signaling

RESULTS

Blocking mSCTs induces homeostatic eEF2 kinase-dependent synaptic scaling

In the next set of experiments, we aimed to examine the physiological impact of RyR-dependent mSCTs by focusing on the putative role of these Ca^{2+} signals in regulation of synaptic efficacy. For this purpose, we investigated the role of mSCTs in homeostatic synaptic scaling, which is a compensatory mechanism where neurons scale the strength of their synaptic inputs multiplicatively in a uniform manner in response to global increases or decreases in activity (Turrigiano, Leslie et al. 1998). This response involves the synthesis and insertion of new AMPA receptors and can be strongly induced by blocking both action potentials and NMDA receptors (Sutton, Wall et al. 2004). Importantly, although synaptic scaling in response to activity blockade occurs within a time frame of 24-48 hrs, suppression of resting synaptic activity mediated by spontaneous neurotransmitter release events results in more rapid synaptic scaling detectable within hours (Sutton, Ito et al. 2006, Nosyreva, Szabla et al. 2013). This suggests that NMDA receptor activation at rest maintains synaptic homeostasis. However, the mechanism by which NMDA receptor activity near resting membrane potentials signals to translation machinery, in particular to eEF2 kinase, has been unclear, especially when one considers

the relatively small ion conductance of NMDA receptors at rest due to Mg^{2+} block (Espinosa and Kavalali 2009).

To investigate the role of RyR-dependent mSCTs in homeostatic synaptic scaling, hippocampal neurons were incubated for 3 hours in culture media containing TTX + vehicle (negative control), TTX + ryanodine, or TTX + AP5 as positive control. Neurons were then perfused with Tyrode's solution and whole cell voltage clamp recordings were made in 1 μM TTX, 50 μM PTX and 50 μM AP5 to isolate AMPA-mEPSCs. Under these conditions, the amplitude distributions of AMPA-mEPSCs obtained from neurons treated previously with TTX + ryanodine as well as those treated with TTX + AP5 showed a significant rightward shift towards larger amplitudes compared to the control condition (Figure 6.1A, B). When the collected mEPSC amplitudes were plotted rank order in control vs TTX + ryanodine, a linear fit revealed a scaling factor of 1.28 indicating that cell-wide, mEPSC amplitudes increased uniformly 28% over 3 hours with TTX + ryanodine treatment (Figure 5C). This increase in mEPSC amplitudes was not as pronounced as was found with the positive control (TTX + AP5) which may correlate with the finding that ryanodine treatment does not block mSCTs as completely as AP5 (figures 4.2D, 4E). It is important to note that while other groups have reported an immediate decrease in mEPSC frequency with the acute application of ryanodine (Emptage, Bliss et al. 1999), in our system the mEPSC frequencies in neurons treated with ryanodine for 15 minutes were indistinguishable from those incubated with vehicle as control (TTX mEPSC freq = 7.59 Hz ± 1.75, TTX + Ryanodine mEPSC freq = 8.92 ± 1.13, $p = 0.54$ using Student's t-test, N = 7 cells from 5 coverslips, 2 cultures). Since the

acute application of ryanodine does not alter mEPSC frequency in this system we believe the synaptic scaling effect mainly results from ryanodine acting at the postsynapse to block mSCT activity.

In earlier experiments homeostatic synaptic scaling that occurs after blockade of resting NMDA receptor activity was shown to rely on protein synthesis, in particular synthesis of new AMPARs rather than the insertion of existing ones (Sutton, Ito et al. 2006, Sutton, Taylor et al. 2007). In order to test whether this is the case for RyR block-induced synaptic scaling, we repeated the experiment above with neurons that were treated with the protein synthesis inhibitor anisomycin (20 μM) starting 30 minutes prior to their 3 hour incubation with TTX. Under these conditions, anisomycin completely abolished the increase in AMPA-mEPSC amplitudes as no significant differences were seen in their distribution after TTX + ryanodine treatment compared to treatment with TTX alone (Figure 6.1D-F).

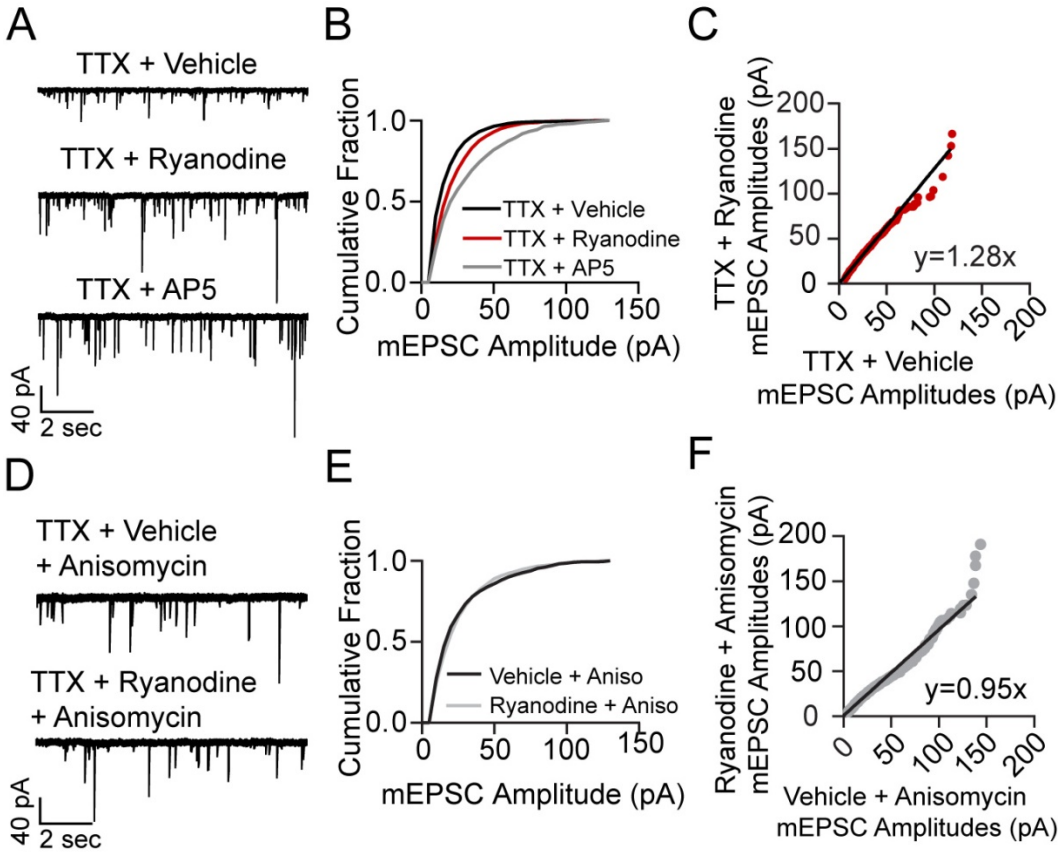

Figure 6.1 – Treating cells with ryanodine + TTX produces a protein synthesis dependent increase in mEPSC frequency and amplitude indicative of homeostatic synaptic scaling

A. Example voltage clamp recordings from cells treated with TTX + vehicle (negative control, N = 9 cells from 5 coverslips, 3 cultures), TTX + ryanodine (N = 8 cells from 5 coverslips, 4 cultures) or TTX + AP5 (positive control, N = 6 cells from 4 coverslips, 2 cultures) for 3 hours. B. Cumulative probability histogram showing significant rightward shifts (increases) in the amplitude of AMPA mEPSCs of cells treated with TTX + ryanodine (red line, $p = 1.74 \times 10^{-17}$, D=0.151), or TTX + AP5 ($p = 8.79 \times 10^{-40}$, D = 0.255) vs control via Kolmogorov-Smirnov test. C. Rank order plot of TTX + vehicle mEPSC amplitudes vs. TTX + ryanodine showing a multiplicative scaling factor of 1.28. D. Example voltage clamp recordings from cells pretreated for 30 minutes with the protein

synthesis inhibitor anisomycin and then TTX + vehicle (N = 6 cells from 5 coverslips, 4 cultures) or TTX + ryanodine for 3 hours (N = 7 cells from 5 coverslips, 2 cultures). E. Cumulative probability histogram of mEPSC amplitudes shows no significant difference between treatment groups when pretreated with anisomycin ($p = 0.078$, $D = 0.052$ via Kolmogorov-Smirnov test). F. Rank order plot of mEPSC amplitudes indicates that anisomycin pretreatment abolishes scaling between treatment groups.

Previous studies have also shown that a key regulator of protein synthesis, eukaryotic elongation factor 2 (eEF2), is phosphorylated and inactivated by the Ca^{2+}-dependent eEF2 kinase thus blocking protein synthesis under resting conditions (Sutton, Taylor et al. 2007, Autry, Adachi et al. 2011, Nosyreva, Szabla et al. 2013, Gideons, Kavalali et al. 2014). To test whether RyR-mediated mSCTs could be tonically activating eEF2 kinase and thus inhibiting protein synthesis in dendrites, we tested the impact of ryanodine treatment in hippocampal neuronal cultures from eEF2 kinase knockout mice. In hippocampal neurons made from wild-type littermate controls, treating with TTX + ryanodine for 3 hours produced a significant increase in mEPSC amplitudes compared to TTX + vehicle, where plotting the amplitudes in rank order revealed a 42% increase in synaptic strength (Figure 6.2A-C). When the same experiment was performed using neurons from eEF2 kinase knockout mice, treatment with TTX + ryanodine did not produce a significant shift in mEPSC amplitudes (Figure 6.2D, E). The rank order plot revealed only a 1% difference in synaptic strength between treatment groups (Figure 6.2F). Taken together these results suggest that RyR-dependent mSCT-driven signaling acts through Ca^{2+}-dependent eEF2 kinase to maintain synaptic homeostasis.

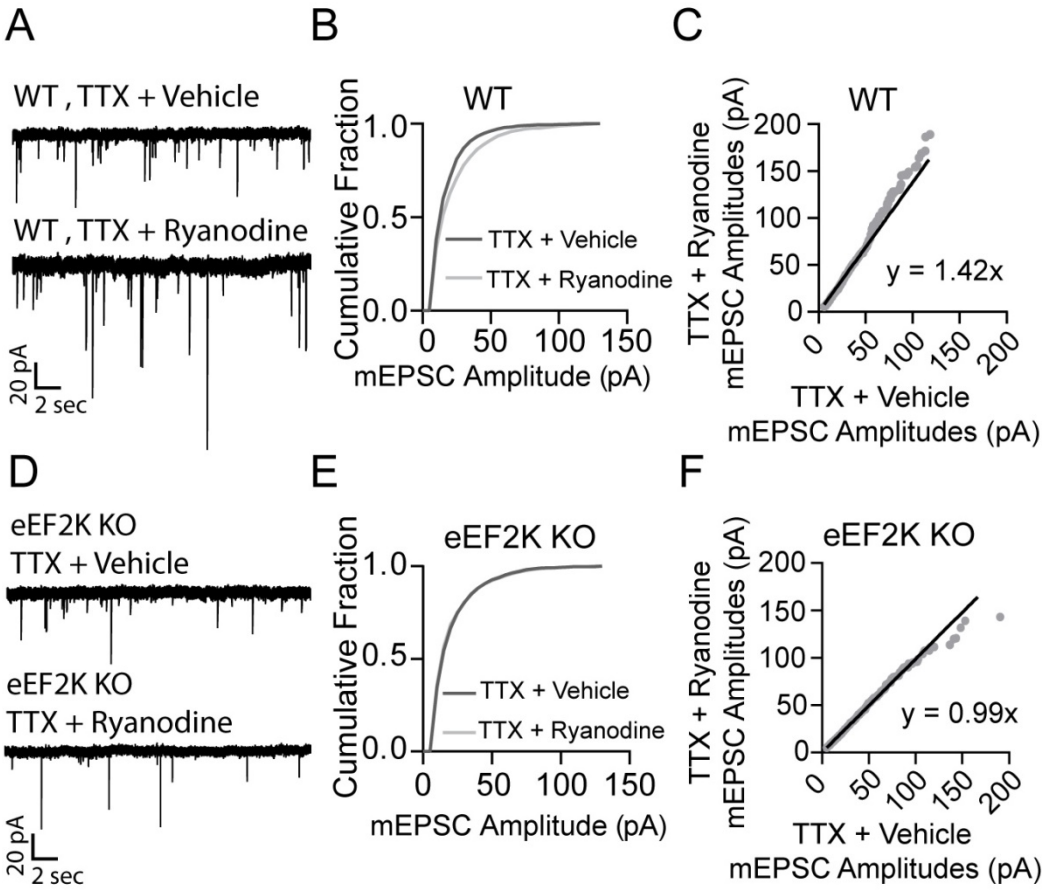

Figure 6.2 - Ryanodine treatment does not trigger homeostatic synaptic scaling in eEF2 kinase knockout neurons.

A. Example traces from WT littermate mice with and without 3 hour ryanodine treatment. B. Cumulative probability histogram shows a significant shift in mEPSC amplitude in TTX + ryanodine treated animals (N = 12 cells, from 7 coverslips, 3 cultures) vs TTX + vehicle control (N = 13 cells from 8 coverslips, 3 cultures) ($p = 3.32 \times 10^{-14}$, D = 0.112 via Kolmogorov-Smirnov test). C. Rank order plot shows a 1.42 fold increase in synaptic strength after ryanodine treatment. D. Example traces from eEF2 kinase KO animals with and without ryanodine treatment. E. Cumulative probability histogram shows no shift in the distribution of mEPSC amplitudes in eEF2K KO animals treated with TTX + ryanodine (N = 9 cells, from 6 coverslips, 3 cultures) vs. TTX + vehicle (N = 13 cells from 7 coverslips, 3 cultures) (p = 0.066, D = 0.058 via

Kolmogorov-Smirnov test). F. Rank order plot shows no appreciable multiplicative change in synaptic strength in the eEF2 K KO animals with ryanodine treatment.

DISCUSSION

In this study, we tested a key prediction of these observations on synaptic plasticity by assessing the role of Ca^{2+}-induced Ca^{2+} release in synaptic scaling triggered at rest. Our experiments showed that the synaptic scaling produced by the blockade of spontaneous NMDA-mEPSCs is also produced by blocking the Ca^{2+} release from internal stores indicating a strong link between the two signals. The generation of relatively large store-driven Ca^{2+} transients provides a critical amplification step for the relatively small NMDA-mEPSCs seen under physiological conditions (Espinosa and Kavalali, 2009; Gideons et al., 2014). The resulting signal is delocalized and pulsatile which may allow synaptic NMDA receptors to exert signaling influence in the surrounding dendritic regions. This could be critical for local translational control as eEF2 localizes to the dendritic shaft rather than dendritic spines (Asaki, Usuda et al. 2003). The low frequency of observed mSCTs may also be a defining attribute, as the ubiquitous Ca^{2+} binding protein calmodulin is predicted to interact with different target kinases and enzymes based on the frequency and duration of its activation by free Ca^{2+} (Saucerman and Bers 2008, Slavov, Carey et al. 2013). Taken together these findings identify a critical missing mechanistic link between spontaneous neurotransmission and the control of dendritic signaling events that regulate synaptic efficacy.

Methods

Whole Cell Voltage Clamp Recordings

Dissociated hippocampal cultures aged 14-18 days *in vitro* were voltage clamped at -70 mV using an Axon Instruments Axopatch 200B amplifier with access resistances less than 25 MΩ for each recording. Internal pipette solution contained (in mM): 120 K-Gluconate, 20 KCl, 10 NaCl, 10 HEPES, 0.6 EGTA, 4 Mg-ATP and 0.3 Na-GTP at pH 7.3. To isolate AMPA-mEPSCs, the extracellular solution contained 1 μM tetrodotoxin (TTX), 50 μM picrotoxin (PTX, to block mIPSCs) and 50 μM (2*R*)-amino-5-phosphonovaleric acid (AP5), 2 mM Ca^{2+} and 1.25 mM Mg^{2+}. All whole cell patch clamp recordings were performed under continuous perfusion. Cells were perfused for 3-minutes prior to recording to achieve stable baselines. No more than 2 recordings were obtained per coverslip.

Whole cell voltage clamp statistics and analysis

AMPA-mEPSCs were quantified using Synaptosoft MiniAnalysis software. Frequency data was collected by quantifying 4 minutes per cell starting at the beginning of each recording. To ensure that high frequency cells did not skew the amplitude comparisons by being over represented, 200 mEPSC amplitudes were randomly selected from each recording to build the cumulative probability histograms and rank order plots.

Kolmogorov-Smirnov test was performed using Past 3.02 (http://folk.uio.no/ohammer/past/).

CHAPTER SEVEN
Further Discussion and Open Questions

Observations surrounding the multiplicative nature of synaptic scaling

Based on the experiments presented here, it's possible to make several inferences about the nature of synaptic homeostasis. My work illustrates a mechanism by which spontaneous NMDAR activity can signal to protein synthesis machinery, although the spatial extent of this signaling is poorly described. Since mSCTs are triggered by spontaneous NMDAR activity at a rate per ROI approaching half that of spontaneous release in general, we can assume that activity at only a single synapse is required to trigger a mSCT. If the input from several spontaneous events were required, the close coincidence of two events would produce a much lower mSCT frequency. Additionally, the observation that mSCTs are both spatially restricted in nature and found throughout the dendritic arbor, points to a mechanism by which synaptic strength might be affected by a local signal.

In experiments where NMDA antagonists were perfused locally, protein synthesis could be stimulated in a single dendritic branch (Sutton, Taylor et al. 2007). However, both these experiments and my own lack single synapse resolution and thus leave open questions about the nature of this effect. First, is it possible that every synapse is competent to modulate its own strength in response to spontaneous activity, or is there a specialized signaling center that controls a cluster of postsynapses? There are indeed Ca^{2+} signaling foci in the dendrites that have been shown to initiate large Ca^{2+} fluxes in the

proximal dendrite that spill into the soma (Hertle and Yeckel 2007). In these foci, IP_3 receptors have been shown to cluster at dendritic branch points where they participate in Ca^{2+} release triggered by VGCCs, NMDARs and mGluR signaling (Nakamura, Lasser-Ross et al. 2002).

RyRs, the receptors critical to controlling synaptic scaling, tend towards differential localization and expression from IP_3Rs (Sharp, McPherson et al. 1993). RyRs localize to ER that is pulled into dendritic spines and may provide localized Ca^{2+} flux in the ~50% of spines that exhibit this structural feature (Spacek and Harris 1997, Korkotian and Segal 1998). Translation of bound transcripts in the dendrite is handled by polyribosome complexes that sit in the dendritic shaft at the base of a dendritic spine. EM studies illustrate that some 29% of hippocampal synapses are associated with such a polyribosome complex (Steward and Levy 1982). Therefore, if spatial proximity is key for the interaction of polyribosome complexes and RyRs, as few as ~15% of all synapses may be poised to control synaptic strength by triggering protein translation for their local region.

Since synaptic scaling is at the very least, autonomous between major dendritic branches and may be controlled in a highly localized manner, this calls into question the multiplicative nature of synaptic scaling itself. A widely accepted idea in neuroscience is that information is stored or encoded into neural circuits as the relative strengths of synaptic connections between relevant neurons (Lisman 1989, Bliss and Collingridge 1993). This explanation integrates the premise of Hebbian learning with observable dynamics in the number and function of synapses resulting from LTP and synaptic

homeostasis. Early descriptions of homeostatic synaptic plasticity provided further support for this hypothesis because of the multiplicative nature of the synaptic changes. By shifting the relative strengths of synapses up or down by a factor rather than by an integer, synaptic scaling preserves the relative differences in strength between synapses and thus the information that is supposedly encoded in those strengths. However, with the notable exception of Sutton and Taylor, 2007, nearly all scaling experiments involve a treatment that suppresses neural activity throughout the entire preparation whether it is a drug treatment in a culture system or input deprivation to visual cortex. In these experiments, the entire cell is affected and thus scales uniformly but it is clearly possible that scaling of a single dendritic branch or a smaller segment is possible. If synaptic scaling is controlled in a localized manner, the ability of a neuron to maintain its relative synaptic weights through homeostatic scaling processes is compromised.

Metaplastic interactions of LTP, LTD and synaptic scaling

If we assume that scaling is not a cell-wide process *in vivo* then it's likely that one or more of the base assumptions is incorrect or incomplete. It may be that the process that we know as homeostatic synaptic plasticity is unlikely to occur in a healthy animal because it upsets synaptic weights. Alternatively, it could be that synaptic weight is only one facet of the information storage mechanism and synaptic scaling does little to upset it but these two ideas do appear at odds. One possible solution to this problem is metaplasticity. The processes thought to set synaptic weights, LTP and LTD, are known

to interact with one another and with themselves to produce complex behaviors that govern the magnitude and time dependence of their actions. In a neural circuit where postsynaptic cells are receiving regular bursts of input, a tetanic stimulation fails to produce LTP indicating that sufficient neural input can occlude LTP (Huang, Colino et al. 1992). The threshold for LTP is in fact dependent on the frequency of tonic input such that a quiescent cell is primed to undergo LTP when a strong stimulation arrives (Bear 1995). The process of LTP is also known to be autoinhibitory in that a cell cannot continuously undergo LTP. The magnitude of the EPSP increase saturates yet this does not represent a maximal strength. A sufficient delay between LTP-inducing stimulation allows further EPSP increases in the same cells, just not in rapid sucession (Frey, Schollmeier et al. 1995). These collective regulation of LTP and LTD are called metaplasticity and are often described as “the plasticity of plasticity” (Abraham and Bear 1996).

It is unproven if LTP occludes synaptic scaling in the same way that it occludes further LTP or perhaps vice versa. One hint may come from studying the NMDA receptor blocker ketamine which is commonly known as a dissociative anesthetic and NMDA receptor blocker. NMDAR block by ketamine produces an effect that appears similar to AP5 induced synaptic scaling and includes an eEF2 dependent increase in EPSP amplitude (Autry, Adachi et al. 2011). Though proper quantification of ketamine driven mEPSC scaling has not been shown, experiments have shown that the presence of ketamine prevents the induction of LTP, presumably because the NMDAR is required for early phase LTP (Zhang and Levy 1992, Malenka 1994). This particular interaction

between presumed synaptic scaling and LTP manifests because NMDAR activity controls both phenomena and acts as a limited resource. However, these results do not preclude further mechanistic interaction of more downstream processes.

Retinoic acid as a functional part of the synaptic scaling process

More recent evidence from the lab of Dr. Lu Chen suggests that the SNARE proteins responsible for trafficking receptors to the postsynaptic membrane after LTP are separate from those utilized in synaptic scaling. By a mechanism that is not yet understood, retinoic acid is synthesized during the synaptic scaling process. In fact, application of retinoic acid seems sufficient to induce synaptic scaling on its own (Arendt, Zhang et al. 2015). The synaptic scaling produced by this application uses a different t-SNARE than LTP to fuse AMPAR containing vesicles to the postsynaptic membrane (syntaxin-3 vs syntaxin-4). Furthermore, the synaptic scaling induced by retinoic acid application is able to occlude further LTP (Arendt, Zhang et al. 2015). It is not yet clear if this retinoic acid dependent mechanism is the same as activity suppression driven synaptic scaling. Retinoic acid application has seemingly novel effects not seen in activity suppression driven scaling such as the rapid suppression of $GABA_A$ currents which generally take multiple days of TTX treatment to observe (Kilman, van Rossum et al. 2002, Sarti, Zhang et al. 2013). Further research is needed to determine if retinoic acid induced scaling is part of the same process as activity suppression induced scaling. The

possibility exists that retinoic acid synthesis represents a concurrent or perhaps later phase of scaling, or may be a parallel yet separate process.

Synaptic scaling and the separation of evoked and spontaneous release

As presented experimentally, there is evidence for the separation of evoked and spontaneous neurotransmission within a single glutamatergic synapse. This may suggest that mEPSC amplitude and EPSC amplitude are capable of scaling separately. The supposed purpose of synaptic scaling to provide input-side control over a cell's firing rate would dictate that the commonly measured mEPSC amplitude increase is accompanied by a similar increase in EPSC amplitude. This is in fact the case in broad terms. TTX induced synaptic scaling produces an EPSC amplitude increase concomitant with the mEPSC amplitude increase after 2-3 days of treatment (Watt, van Rossum et al. 2000). The fact remains that single synapses measurements have not been made and significant deviations among individual synapses may illuminate finer control of these parameters. This raises several questions about the nature of receptors trafficking to synapses. If AMPARs are separated into evoked and spontaneous responding pools, are these receptors delivered to the synapse under one mechanism or perhaps delivered separately? These questions can also be extrapolated to apply to the delivery of AMPARs and NMDARs, which seem to maintain their ratio after synaptic perturbation (Watt, van Rossum et al. 2000). In the case of LTP, however, AMPARs are rapidly delivered to the synapse to increase EPSC amplitude quickly, while NMDAR appearance at potentiated

synapses lags behind by some 2 hours (Watt, Sjostrom et al. 2004). This result suggests separate delivery systems for the two sets of receptors. In the case of synaptic scaling, a proper timelapse of NMDA receptor delivery has not been measured.

Throughout this chapter, most of the questions posed remain unanswered due to the lack of single-synapse measurements. Going forward, optical techniques will be key tools in elucidating the parameters controlling the processes of synaptic scaling and LTP/LTD. In the case of chapter 2, the ability of MK-801 to block spontaneous but not evoked NMDA responses had been previously described but modern optical techniques have allowed for measurement of this phenomenon at the single synapse level. By using GCaMP6f-PSD95, I have been able to confirm that evoked and spontaneous transmission occupy the same synapses yet segregate their NMDARs; something that was not possible by electrophysiological methods. It is my prediction and my hope that single-synapse optical techniques will be able to answer many of the questions laid out in this chapter, bringing insight and control over the neural processes that balance network activity and maintain healthy function in the brain.

APPENDIX A
Supplementary figures

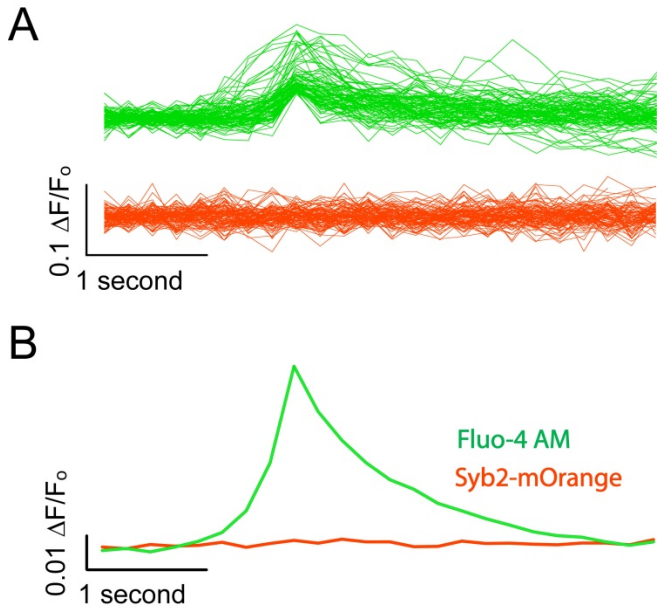

Figure 4.2 supplement 1 – Syb2-mOrange fluorescence does not contaminate Fluo-4 AM signals

A. Example traces from simultaneous Fluo-4 AM / synaptobrevin-mOrange imaging. Cells were imaged alternating the excitation between Fluo-4 AM and Syb2-mO for every other frame. Each frame was exposed for 100 ms as described previously and frames were collected at 5 fps per channel. Events were detected as described previously using the Fluo-4 AM channel and the data for both wavelengths was aligned to the peak value in the green channel. Green traces show example evens detected in the channel excited with 470±40 nm light to excite Fluo-4 AM and the red traces show the corresponding data collected with a 548±10 nm excitation filter to excite Syb2-mOrange.

B. Average traces made from 382 detected and aligned events. The average trace in the Fluo-4 AM channel shows a robust Ca^{2+} transient while the averaged Syb2-mO data shows no appreciable deviation from baseline.

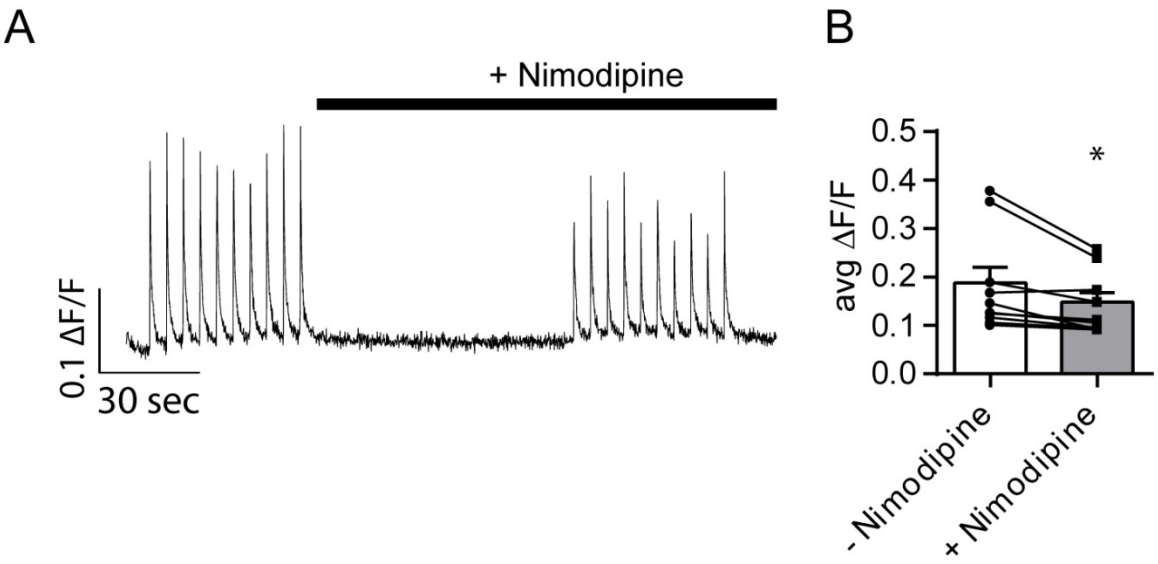

Figure 4.4, supplement 1 - Nimodipine produces positive results in a separate assay

A. Example traces showing Ca^{2+} influx during action potentials in the absence and presence of nimodipine. Cells were loaded with Fluo-4 AM and imaged in Tyrode's solution containing 1.25 mM Mg^{2+}, 2 mM Ca^{2+}, 50 µM AP5 and 20 µM NBQX. 10 action potentials were evoked via field stimulation at 0.2 Hz. Then, the perfusion was changed to include 5µM of the L-type calcium channel blocker nimodipine for 1 minute before repeating the stimulation. ROIs were 20 µm in diameter placed on the cell soma. B. Average peak fluorescence from action potential trains before and after the addition of 5 µM nimodipine. The addition of nimodipine restricts Ca^{2+} influx during the action potential by ~27%. N = 8 cells, 1 culture. p = 0.019 via Student's paired t-test.

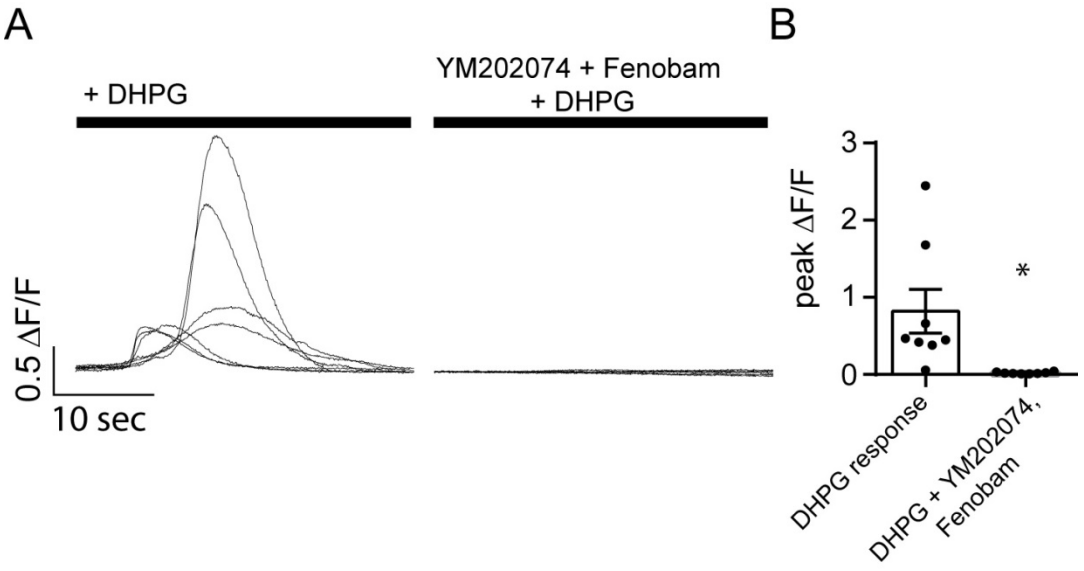

Figure 4.4, supplement 2 – YM202074 and Fenobam produce positive results in a separate assay

A. Cells loaded with Fluo-4 AM were imaged in Tyrode's solution containing 1.25 mM Mg^{2+}, 2 mM Ca^{2+} and TTX with or without the mGluR1/5 blockers YM202074 and fenobam. The solution was then changed to include 100 μM DHPG (a mGluR1/5 agonist) where it elicited large slow Ca^{2+} influx in the cells not treated with YM202074 and fenobam. B. Peak ΔF/F measurements for the experiment described in panel C shows marked inhibition of the DHPG response in cells treated with mGluR1/5 antagonists. p = 0.015 via Student's t-test. N =8 cells per group from 8 coverslips, 1 culture.

BIBLIOGRAPHY

Abenavoli, A., L. Forti, M. Bossi, A. Bergamaschi, A. Villa and A. Malgaroli (2002). "Multimodal quantal release at individual hippocampal synapses: evidence for no lateral inhibition." J Neurosci **22**(15): 6336-6346.

Abraham, W. C. and M. F. Bear (1996). "Metaplasticity: the plasticity of synaptic plasticity." Trends Neurosci **19**(4): 126-130.

Ahern, G. P., P. R. Junankar and A. F. Dulhunty (1997). "Subconductance states in single-channel activity of skeletal muscle ryanodine receptors after removal of FKBP12." Biophys J **72**(1): 146-162.

Akerboom, J., T. W. Chen, T. J. Wardill, L. Tian, J. S. Marvin, S. Mutlu, N. C. Calderon, F. Esposti, B. G. Borghuis, X. R. Sun, A. Gordus, M. B. Orger, R. Portugues, F. Engert, J. J. Macklin, A. Filosa, A. Aggarwal, R. A. Kerr, R. Takagi, S. Kracun, E. Shigetomi, B. S. Khakh, H. Baier, L. Lagnado, S. S. Wang, C. I. Bargmann, B. E. Kimmel, V. Jayaraman, K. Svoboda, D. S. Kim, E. R. Schreiter and L. L. Looger (2012). "Optimization of a GCaMP calcium indicator for neural activity imaging." J Neurosci **32**(40): 13819-13840.

Amador, F. J., S. Liu, N. Ishiyama, M. J. Plevin, A. Wilson, D. H. MacLennan and M. Ikura (2009). "Crystal structure of type I ryanodine receptor amino-terminal beta-trefoil domain reveals a disease-associated mutation "hot spot" loop." Proc Natl Acad Sci U S A **106**(27): 11040-11044.

Aoto, J., C. I. Nam, M. M. Poon, P. Ting and L. Chen (2008). "Synaptic signaling by all-trans retinoic acid in homeostatic synaptic plasticity." Neuron **60**(2): 308-320.

Arendt, K. L., Y. Zhang, S. Jurado, R. C. Malenka, T. C. Sudhof and L. Chen (2015). "Retinoic Acid and LTP Recruit Postsynaptic AMPA Receptors Using Distinct SNARE-Dependent Mechanisms." Neuron **86**(2): 442-456.

Arendt, K. L., Z. Zhang, S. Ganesan, M. Hintze, M. M. Shin, Y. Tang, A. Cho, I. A. Graef and L. Chen (2015). "Calcineurin mediates homeostatic synaptic plasticity by regulating retinoic acid synthesis." Proc Natl Acad Sci U S A **112**(42): E5744-5752.

Asaki, C., N. Usuda, A. Nakazawa, K. Kametani and T. Suzuki (2003). "Localization of translational components at the ultramicroscopic level at postsynaptic sites of the rat brain." Brain Res **972**(1-2): 168-176.

Atasoy, D., M. Ertunc, K. L. Moulder, J. Blackwell, C. Chung, J. Su and E. T. Kavalali (2008). "Spontaneous and evoked glutamate release activates two populations of NMDA receptors with limited overlap." J Neurosci **28**(40): 10151-10166.

Autry, A. E., M. Adachi, E. Nosyreva, E. S. Na, M. F. Los, P. F. Cheng, E. T. Kavalali and L. M. Monteggia (2011). "NMDA receptor blockade at rest triggers rapid behavioural antidepressant responses." Nature **475**(7354): 91-95.

Bear, M. F. (1995). "Mechanism for a sliding synaptic modification threshold." Neuron **15**(1): 1-4.

Bekkers, J. M. and C. F. Stevens (1989). "NMDA and non-NMDA receptors are co-localized at individual excitatory synapses in cultured rat hippocampus." Nature **341**(6239): 230-233.

Bezprozvanny, I., J. Watras and B. E. Ehrlich (1991). "Bell-shaped calcium-response curves of Ins(1,4,5)P3- and calcium-gated channels from endoplasmic reticulum of cerebellum." Nature **351**(6329): 751-754.

Bliss, T. V. and G. L. Collingridge (1993). "A synaptic model of memory: long-term potentiation in the hippocampus." Nature **361**(6407): 31-39.

Bloodgood, B. L. and B. L. Sabatini (2005). "Neuronal activity regulates diffusion across the neck of dendritic spines." Science **310**(5749): 866-869.

Borges, K. and R. Dingledine (1998). "AMPA receptors: molecular and functional diversity." Prog Brain Res **116**: 153-170.

Brillantes, A. B., K. Ondrias, A. Scott, E. Kobrinsky, E. Ondriasova, M. C. Moschella, T. Jayaraman, M. Landers, B. E. Ehrlich and A. R. Marks (1994). "Stabilization of calcium release channel (ryanodine receptor) function by FK506-binding protein." Cell **77**(4): 513-523.

Bronk, P., F. Deak, M. C. Wilson, X. Liu, T. C. Sudhof and E. T. Kavalali (2007). "Differential effects of SNAP-25 deletion on Ca2+ -dependent and Ca2+ -independent neurotransmission." J Neurophysiol **98**(2): 794-806.

Capes, E. M., R. Loaiza and H. H. Valdivia (2011). "Ryanodine receptors." Skelet Muscle **1**(1): 18.

Chavis, P., L. Fagni, J. B. Lansman and J. Bockaert (1996). "Functional coupling between ryanodine receptors and L-type calcium channels in neurons." Nature **382**(6593): 719-722.

Chen, Y., Y. Wang, Z. Modrusan, M. Sheng and J. S. Kaminker (2014). "Regulation of Neuronal Gene Expression and Survival by Basal NMDA Receptor Activity: A Role for Histone Deacetylase 4." J Neurosci **34**(46): 15327-15339.

Christie, B. R., L. S. Eliot, K. Ito, H. Miyakawa and D. Johnston (1995). "Different Ca2+ channels in soma and dendrites of hippocampal pyramidal neurons mediate spike-induced Ca2+ influx." J Neurophysiol **73**(6): 2553-2557.

Chung, C. and E. T. Kavalali (2006). "Seeking a function for spontaneous neurotransmission." Nat Neurosci **9**(8): 989-990.

Colman, H., J. Nabekura and J. W. Lichtman (1997). "Alterations in synaptic strength preceding axon withdrawal." Science **275**(5298): 356-361.

Ebashi, S. and F. Lipmann (1962). "Adenosine triphosphate-linked concentration of calcium ions in a particulate fraction of rabbit muscle." Biochem Biophys Res Commun **369**(1): 1-12.

Elliott, E. M. and R. M. Sapolsky (1993). "Corticosterone impairs hippocampal neuronal calcium regulation--possible mediating mechanisms." Brain Res **602**(1): 84-90.

Emptage, N., T. V. Bliss and A. Fine (1999). "Single synaptic events evoke NMDA receptor-mediated release of calcium from internal stores in hippocampal dendritic spines." Neuron **22**(1): 115-124.

Espinosa, F. and E. T. Kavalali (2009). "NMDA receptor activation by spontaneous glutamatergic neurotransmission." J Neurophysiol **101**(5): 2290-2296.

Fatt, P. and B. Katz (1952). "Spontaneous subthreshold activity at motor nerve endings." J Physiol **117**(1): 109-128.

Fisher, R. E., R. Gray and D. Johnston (1990). "Properties and distribution of single voltage-gated calcium channels in adult hippocampal neurons." J Neurophysiol **64**(1): 91-104.

Fredj, N. B. and J. Burrone (2009). "A resting pool of vesicles is responsible for spontaneous vesicle fusion at the synapse." Nat Neurosci **12**(6): 751-758.

Frey, U., K. Schollmeier, K. G. Reymann and T. Seidenbecher (1995). "Asymptotic hippocampal long-term potentiation in rats does not preclude additional potentiation at later phases." Neuroscience **67**(4): 799-807.

Fruen, B. R., J. R. Mickelson and C. F. Louis (1997). "Dantrolene inhibition of sarcoplasmic reticulum Ca2+ release by direct and specific action at skeletal muscle ryanodine receptors." J Biol Chem **272**(43): 26965-26971.

Furuichi, T., K. Kohda, A. Miyawaki and K. Mikoshiba (1994). "Intracellular channels." Curr Opin Neurobiol **4**(3): 294-303.

Gee, K. R., K. A. Brown, W. N. Chen, J. Bishop-Stewart, D. Gray and I. Johnson (2000). "Chemical and physiological characterization of fluo-4 Ca(2+)-indicator dyes." Cell Calcium **27**(2): 97-106.

Giannini, G., A. Conti, S. Mammarella, M. Scrobogna and V. Sorrentino (1995). "The ryanodine receptor/calcium channel genes are widely and differentially expressed in murine brain and peripheral tissues." J Cell Biol **128**(5): 893-904.

Gideons, E. S., E. T. Kavalali and L. M. Monteggia (2014). "Mechanisms underlying differential effectiveness of memantine and ketamine in rapid antidepressant responses." Proc Natl Acad Sci U S A **111**(23): 8649-8654.

Guire, E. S., M. C. Oh, T. R. Soderling and V. A. Derkach (2008). "Recruitment of calcium-permeable AMPA receptors during synaptic potentiation is regulated by CaM-kinase I." J Neurosci **28**(23): 6000-6009.

Harnett, M. T., J. K. Makara, N. Spruston, W. L. Kath and J. C. Magee (2012). "Synaptic amplification by dendritic spines enhances input cooperativity." Nature **491**(7425): 599-602.

Hashii, M., Y. Minabe and H. Higashida (2000). "cADP-ribose potentiates cytosolic Ca2+ elevation and Ca2+ entry via L-type voltage-activated Ca2+ channels in NG108-15 neuronal cells." Biochem J **345 Pt 2**: 207-215.

Hawkes, M. J., T. E. Nelson and S. L. Hamilton (1992). "[3H]ryanodine as a probe of changes in the functional state of the Ca(2+)-release channel in malignant hyperthermia." J Biol Chem **267**(10): 6702-6709.

Hertle, D. N. and M. F. Yeckel (2007). "Distribution of inositol-1,4,5-trisphosphate receptor isotypes and ryanodine receptor isotypes during maturation of the rat hippocampus." Neuroscience **150**(3): 625-638.

Hollmann, M., M. Hartley and S. Heinemann (1991). "Ca2+ permeability of KA-AMPA--gated glutamate receptor channels depends on subunit composition." Science **252**(5007): 851-853.

Huang, Y. Y., A. Colino, D. K. Selig and R. C. Malenka (1992). "The influence of prior synaptic activity on the induction of long-term potentiation." Science **255**(5045): 730-733.

Hughes, S. J., H. Smith and S. J. Ashcroft (1993). "Characterization of Ca2+/calmodulin-dependent protein kinase in rat pancreatic islets." Biochem J **289 (Pt 3)**: 795-800.

Ikemoto, T., H. Takeshima, M. Iino and M. Endo (1998). "Effect of calmodulin on Ca2+-induced Ca2+ release of skeletal muscle from mutant mice expressing either ryanodine receptor type 1 or type 3." Pflugers Arch **437**(1): 43-48.

Jaffe, D. B., D. Johnston, N. Lasser-Ross, J. E. Lisman, H. Miyakawa and W. N. Ross (1992). "The spread of Na+ spikes determines the pattern of dendritic Ca2+ entry into hippocampal neurons." Nature **357**(6375): 244-246.

Jahr, C. E. and C. F. Stevens (1990). "Voltage dependence of NMDA-activated macroscopic conductances predicted by single-channel kinetics." J Neurosci **10**(9): 3178-3182.

Jorquera, R. A., S. Huntwork-Rodriguez, Y. Akbergenova, R. W. Cho and J. T. Littleton (2012). "Complexin controls spontaneous and evoked neurotransmitter release by regulating the timing and properties of synaptotagmin activity." J Neurosci **32**(50): 18234-18245.

Ju, W., W. Morishita, J. Tsui, G. Gaietta, T. J. Deerinck, S. R. Adams, C. C. Garner, R. Y. Tsien, M. H. Ellisman and R. C. Malenka (2004). "Activity-dependent regulation of dendritic synthesis and trafficking of AMPA receptors." Nat Neurosci **7**(3): 244-253.

Kavalali, E. T. (2014). "The mechanisms and functions of spontaneous neurotransmitter release." Nat Rev Neurosci **16**(1): 5-16.

Kavalali, E. T., J. Klingauf and R. W. Tsien (1999). "Activity-dependent regulation of synaptic clustering in a hippocampal culture system." Proc Natl Acad Sci U S A **96**(22): 12893-12900.

Kavalali, E. T. and M. R. Plummer (1996). "Multiple voltage-dependent mechanisms potentiate calcium channel activity in hippocampal neurons." J Neurosci **16**(3): 1072-1082.

Kerr, A. M., E. Reisinger and P. Jonas (2008). "Differential dependence of phasic transmitter release on synaptotagmin 1 at GABAergic and glutamatergic hippocampal synapses." Proc Natl Acad Sci U S A **105**(40): 15581-15586.

Kilman, V., M. C. van Rossum and G. G. Turrigiano (2002). "Activity deprivation reduces miniature IPSC amplitude by decreasing the number of postsynaptic GABA(A) receptors clustered at neocortical synapses." J Neurosci **22**(4): 1328-1337.

Korkotian, E. and M. Segal (1998). "Fast confocal imaging of calcium released from stores in dendritic spines." Eur J Neurosci **10**(6): 2076-2084.

Kovalchuk, Y., J. Eilers, J. Lisman and A. Konnerth (2000). "NMDA receptor-mediated subthreshold Ca(2+) signals in spines of hippocampal neurons." J Neurosci **20**(5): 1791-1799.

Lalonde, J., G. Saia and G. Gill (2014). "Store-operated calcium entry promotes the degradation of the transcription factor Sp4 in resting neurons." Sci Signal **7**(328): ra51.

Larkum, M. E., S. Watanabe, T. Nakamura, N. Lasser-Ross and W. N. Ross (2003). "Synaptically activated Ca2+ waves in layer 2/3 and layer 5 rat neocortical pyramidal neurons." J Physiol **549**(Pt 2): 471-488.

Lei, S. Z., D. Zhang, A. E. Abele and S. A. Lipton (1992). "Blockade of NMDA receptor-mediated mobilization of intracellular Ca2+ prevents neurotoxicity." Brain Res **598**(1-2): 196-202.

Leitz, J. and E. Kavalali (2014). "Fast retrieval and autonomous regulation of single spontaneously recycling synaptic vesicles." Elife **3**.

Liao, D., R. H. Scannevin and R. Huganir (2001). "Activation of silent synapses by rapid activity-dependent synaptic recruitment of AMPA receptors." J Neurosci **21**(16): 6008-6017.

Lisman, J. (1989). "A mechanism for the Hebb and the anti-Hebb processes underlying learning and memory." Proc Natl Acad Sci U S A **86**(23): 9574-9578.

Magee, J. C., R. B. Avery, B. R. Christie and D. Johnston (1996). "Dihydropyridine-sensitive, voltage-gated Ca2+ channels contribute to the resting intracellular Ca2+ concentration of hippocampal CA1 pyramidal neurons." J Neurophysiol **76**(5): 3460-3470.

Magee, J. C., G. Christofi, H. Miyakawa, B. Christie, N. Lasser-Ross and D. Johnston (1995). "Subthreshold synaptic activation of voltage-gated Ca2+ channels mediates a localized Ca2+ influx into the dendrites of hippocampal pyramidal neurons." J Neurophysiol **74**(3): 1335-1342.

Maghsoodi, B., M. M. Poon, C. I. Nam, J. Aoto, P. Ting and L. Chen (2008). "Retinoic acid regulates RARalpha-mediated control of translation in dendritic RNA granules during homeostatic synaptic plasticity." Proc Natl Acad Sci U S A **105**(41): 16015-16020.

Malenka, R. C. (1994). "Synaptic plasticity in the hippocampus: LTP and LTD." Cell **78**(4): 535-538.

Marqueze, B., J. A. Boudier, M. Mizuta, N. Inagaki, S. Seino and M. Seagar (1995). "Cellular localization of synaptotagmin I, II, and III mRNAs in the central nervous system and pituitary and adrenal glands of the rat." J Neurosci **15**(7 Pt 1): 4906-4917.

Marx, S. O., S. Reiken, Y. Hisamatsu, T. Jayaraman, D. Burkhoff, N. Rosemblit and A. R. Marks (2000). "PKA phosphorylation dissociates FKBP12.6 from the calcium release channel (ryanodine receptor): defective regulation in failing hearts." Cell **101**(4): 365-376.

Maximov, A., J. Tang, X. Yang, Z. P. Pang and T. C. Sudhof (2009). "Complexin controls the force transfer from SNARE complexes to membranes in fusion." Science **323**(5913): 516-521.

McMahon, H. T., M. Missler, C. Li and T. C. Sudhof (1995). "Complexins: cytosolic proteins that regulate SNAP receptor function." Cell **83**(1): 111-119.

Meissner, G. and A. el-Hashem (1992). "Ryanodine as a functional probe of the skeletal muscle sarcoplasmic reticulum Ca2+ release channel." Mol Cell Biochem **114**(1-2): 119-123.

Melom, J. E., Y. Akbergenova, J. P. Gavornik and J. T. Littleton (2013). "Spontaneous and evoked release are independently regulated at individual active zones." J Neurosci **33**(44): 17253-17263.

Meszaros, L. G., J. Bak and A. Chu (1993). "Cyclic ADP-ribose as an endogenous regulator of the non-skeletal type ryanodine receptor Ca2+ channel." Nature **364**(6432): 76-79.

Miyakawa, T., A. Mizushima, K. Hirose, T. Yamazawa, I. Bezprozvanny, T. Kurosaki and M. Iino (2001). "Ca(2+)-sensor region of IP(3) receptor controls intracellular Ca(2+) signaling." EMBO J **20**(7): 1674-1680.

Naisbitt, S., E. Kim, J. C. Tu, B. Xiao, C. Sala, J. Valtschanoff, R. J. Weinberg, P. F. Worley and M. Sheng (1999). "Shank, a novel family of postsynaptic density proteins that binds to the NMDA receptor/PSD-95/GKAP complex and cortactin." Neuron **23**(3): 569-582.

Nakamura, T., N. Lasser-Ross, K. Nakamura and W. N. Ross (2002). "Spatial segregation and interaction of calcium signalling mechanisms in rat hippocampal CA1 pyramidal neurons." J Physiol **543**(Pt 2): 465-480.

Nosyreva, E., K. Szabla, A. E. Autry, A. G. Ryazanov, L. M. Monteggia and E. T. Kavalali (2013). "Acute suppression of spontaneous neurotransmission drives synaptic potentiation." J Neurosci **33**(16): 6990-7002.

Orlova, E. V., Serysheva, II, M. van Heel, S. L. Hamilton and W. Chiu (1996). "Two structural configurations of the skeletal muscle calcium release channel." Nat Struct Biol **3**(6): 547-552.

Parker, I. and Y. Yao (1991). "Regenerative release of calcium from functionally discrete subcellular stores by inositol trisphosphate." Proc Biol Sci **246**(1317): 269-274.

Peled, E. S., Z. L. Newman and E. Y. Isacoff (2014). "Evoked and spontaneous transmission favored by distinct sets of synapses." Curr Biol **24**(5): 484-493.

Plummer, M. R., D. E. Logothetis and P. Hess (1989). "Elementary properties and pharmacological sensitivities of calcium channels in mammalian peripheral neurons." Neuron **2**(5): 1453-1463.

Popovic, M. A., X. Gao, N. T. Carnevale and D. Zecevic (2014). "Cortical dendritic spine heads are not electrically isolated by the spine neck from membrane potential signals in parent dendrites." Cereb Cortex **24**(2): 385-395.

Povysheva, N. V. and J. W. Johnson (2012). "Tonic NMDA receptor-mediated current in prefrontal cortical pyramidal cells and fast-spiking interneurons." J Neurophysiol **107**(8): 2232-2243.

Ramirez, D. M., M. Khvotchev, B. Trauterman and E. T. Kavalali (2012). "Vti1a identifies a vesicle pool that preferentially recycles at rest and maintains spontaneous neurotransmission." Neuron **73**(1): 121-134.

Reese, A. L. and E. T. Kavalali (2015). "Spontaneous neurotransmission signals through store-driven Ca(2+) transients to maintain synaptic homeostasis." Elife **4**.

Rosenmund, C. and C. F. Stevens (1996). "Definition of the readily releasable pool of vesicles at hippocampal synapses." Neuron **16**(6): 1197-1207.

Rothschuh, K. E. (1973). History of physiology, Krieger Pub Co.

Sabatini, B. L. and K. Svoboda (2000). "Analysis of calcium channels in single spines using optical fluctuation analysis." Nature **408**(6812): 589-593.

Sandler, V. M. and J. G. Barbara (1999). "Calcium-induced calcium release contributes to action potential-evoked calcium transients in hippocampal CA1 pyramidal neurons." J Neurosci **19**(11): 4325-4336.

Sara, Y., T. Virmani, F. Deak, X. Liu and E. T. Kavalali (2005). "An isolated pool of vesicles recycles at rest and drives spontaneous neurotransmission." Neuron **45**(4): 563-573.

Sarti, F., Z. Zhang, J. Schroeder and L. Chen (2013). "Rapid suppression of inhibitory synaptic transmission by retinoic acid." J Neurosci **33**(28): 11440-11450.

Saucerman, J. J. and D. M. Bers (2008). "Calmodulin mediates differential sensitivity of CaMKII and calcineurin to local Ca2+ in cardiac myocytes." Biophys J **95**(10): 4597-4612.

Schiefer, A., G. Meissner and G. Isenberg (1995). "Ca2+ activation and Ca2+ inactivation of canine reconstituted cardiac sarcoplasmic reticulum Ca(2+)-release channels." J Physiol **489 (Pt 2)**: 337-348.

Schoch, S., F. Deak, A. Konigstorfer, M. Mozhayeva, Y. Sara, T. C. Sudhof and E. T. Kavalali (2001). "SNARE function analyzed in synaptobrevin/VAMP knockout mice." Science **294**(5544): 1117-1122.

Sharp, A. H., P. S. McPherson, T. M. Dawson, C. Aoki, K. P. Campbell and S. H. Snyder (1993). "Differential immunohistochemical localization of inositol 1,4,5-trisphosphate- and ryanodine-sensitive Ca2+ release channels in rat brain." J Neurosci **13**(7): 3051-3063.

Shigemoto, R., A. Kinoshita, E. Wada, S. Nomura, H. Ohishi, M. Takada, P. J. Flor, A. Neki, T. Abe, S. Nakanishi and N. Mizuno (1997). "Differential presynaptic localization of metabotropic glutamate receptor subtypes in the rat hippocampus." J Neurosci **17**(19): 7503-7522.

Skeberdis, V. A., J. Lan, T. Opitz, X. Zheng, M. V. Bennett and R. S. Zukin (2001). "mGluR1-mediated potentiation of NMDA receptors involves a rise in intracellular calcium and activation of protein kinase C." Neuropharmacology **40**(7): 856-865.

Slavov, N., J. Carey and S. Linse (2013). "Calmodulin transduces Ca2+ oscillations into differential regulation of its target proteins." ACS Chem Neurosci **4**(4): 601-612.

Sonnleitner, A., A. Conti, F. Bertocchini, H. Schindler and V. Sorrentino (1998). "Functional properties of the ryanodine receptor type 3 (RyR3) Ca2+ release channel." EMBO J **17**(10): 2790-2798.

Spacek, J. and K. M. Harris (1997). "Three-dimensional organization of smooth endoplasmic reticulum in hippocampal CA1 dendrites and dendritic spines of the immature and mature rat." J Neurosci **17**(1): 190-203.

Steward, O. and W. B. Levy (1982). "Preferential localization of polyribosomes under the base of dendritic spines in granule cells of the dentate gyrus." J Neurosci **2**(3): 284-291.

Sudhof, T. C. (2004). "The synaptic vesicle cycle." Annu Rev Neurosci **27**: 509-547.

Sutton, M. A., H. T. Ito, P. Cressy, C. Kempf, J. C. Woo and E. M. Schuman (2006). "Miniature neurotransmission stabilizes synaptic function via tonic suppression of local dendritic protein synthesis." Cell **125**(4): 785-799.

Sutton, M. A., A. M. Taylor, H. T. Ito, A. Pham and E. M. Schuman (2007). "Postsynaptic decoding of neural activity: eEF2 as a biochemical sensor coupling miniature synaptic transmission to local protein synthesis." Neuron **55**(4): 648-661.

Sutton, M. A., N. R. Wall, G. N. Aakalu and E. M. Schuman (2004). "Regulation of dendritic protein synthesis by miniature synaptic events." Science **304**(5679): 1979-1983.

Swanson, G. T., S. K. Kamboj and S. G. Cull-Candy (1997). "Single-channel properties of recombinant AMPA receptors depend on RNA editing, splice variation, and subunit composition." J Neurosci **17**(1): 58-69.

Tafoya, L. C., M. Mameli, T. Miyashita, J. F. Guzowski, C. F. Valenzuela and M. C. Wilson (2006). "Expression and function of SNAP-25 as a universal SNARE component in GABAergic neurons." J Neurosci **26**(30): 7826-7838.

Takamori, S., M. Holt, K. Stenius, E. A. Lemke, M. Gronborg, D. Riedel, H. Urlaub, S. Schenck, B. Brugger, P. Ringler, S. A. Muller, B. Rammner, F. Grater, J. S. Hub, B. L. De Groot, G. Mieskes, Y. Moriyama, J. Klingauf, H. Grubmuller, J. Heuser, F. Wieland and R. Jahn (2006). "Molecular anatomy of a trafficking organelle." Cell **127**(4): 831-846.

Tang, J., A. Maximov, O. H. Shin, H. Dai, J. Rizo and T. C. Sudhof (2006). "A complexin/synaptotagmin 1 switch controls fast synaptic vesicle exocytosis." Cell **126**(6): 1175-1187.

Topolnik, L., M. Azzi, F. Morin, A. Kougioumoutzakis and J. C. Lacaille (2006). "mGluR1/5 subtype-specific calcium signalling and induction of long-term potentiation in rat hippocampal oriens/alveus interneurones." J Physiol **575**(Pt 1): 115-131.

Tripathy, A., L. Xu, G. Mann and G. Meissner (1995). "Calmodulin activation and inhibition of skeletal muscle Ca2+ release channel (ryanodine receptor)." Biophys J **69**(1): 106-119.

Tu, J. C., B. Xiao, S. Naisbitt, J. P. Yuan, R. S. Petralia, P. Brakeman, A. Doan, V. K. Aakalu, A. A. Lanahan, M. Sheng and P. F. Worley (1999). "Coupling of mGluR/Homer and PSD-95 complexes by the Shank family of postsynaptic density proteins." Neuron **23**(3): 583-592.

Tu, J. C., B. Xiao, J. P. Yuan, A. A. Lanahan, K. Leoffert, M. Li, D. J. Linden and P. F. Worley (1998). "Homer binds a novel proline-rich motif and links group 1 metabotropic glutamate receptors with IP3 receptors." Neuron **21**(4): 717-726.

Turrigiano, G. G., K. R. Leslie, N. S. Desai, L. C. Rutherford and S. B. Nelson (1998). "Activity-dependent scaling of quantal amplitude in neocortical neurons." Nature **391**(6670): 892-896.

Van Amsterdam, F. T. and J. Zaagsma (1986). "Modulation of ATP-dependent calcium extrusion and Na+/Ca2+ exchange across rat cardiac sarcolemma by calcium antagonists." Eur J Pharmacol **123**(3): 441-449.

Verkhratsky, A. and A. Shmigol (1996). "Calcium-induced calcium release in neurones." Cell Calcium **19**(1): 1-14.

Vissavajjhala, P., W. G. Janssen, Y. Hu, A. H. Gazzaley, T. Moran, P. R. Hof and J. H. Morrison (1996). "Synaptic distribution of the AMPA-GluR2 subunit and its colocalization with calcium-binding proteins in rat cerebral cortex: an immunohistochemical study using a GluR2-specific monoclonal antibody." Exp Neurol **142**(2): 296-312.

Wakui, M., B. V. Potter and O. H. Petersen (1989). "Pulsatile intracellular calcium release does not depend on fluctuations in inositol trisphosphate concentration." Nature **339**(6222): 317-320.

Wang, H. L., Z. Zhang, M. Hintze and L. Chen (2011). "Decrease in calcium concentration triggers neuronal retinoic acid synthesis during homeostatic synaptic plasticity." J Neurosci **31**(49): 17764-17771.

Washbourne, P., P. M. Thompson, M. Carta, E. T. Costa, J. R. Mathews, G. Lopez-Bendito, Z. Molnar, M. W. Becher, C. F. Valenzuela, L. D. Partridge and M. C. Wilson (2002). "Genetic ablation of the t-SNARE SNAP-25 distinguishes mechanisms of neuroexocytosis." Nat Neurosci **5**(1): 19-26.

Washburn, M. S., M. Numberger, S. Zhang and R. Dingledine (1997). "Differential dependence on GluR2 expression of three characteristic features of AMPA receptors." J Neurosci **17**(24): 9393-9406.

Watt, A. J., P. J. Sjostrom, M. Hausser, S. B. Nelson and G. G. Turrigiano (2004). "A proportional but slower NMDA potentiation follows AMPA potentiation in LTP." Nat Neurosci **7**(5): 518-524.

Watt, A. J., M. C. van Rossum, K. M. MacLeod, S. B. Nelson and G. G. Turrigiano (2000). "Activity coregulates quantal AMPA and NMDA currents at neocortical synapses." Neuron **26**(3): 659-670.

Weber, T., B. V. Zemelman, J. A. McNew, B. Westermann, M. Gmachl, F. Parlati, T. H. Sollner and J. E. Rothman (1998). "SNAREpins: minimal machinery for membrane fusion." Cell **92**(6): 759-772.

Yang, X., P. Cao and T. C. Sudhof (2013). "Deconstructing complexin function in activating and clamping Ca2+-triggered exocytosis by comparing knockout and knockdown phenotypes." Proc Natl Acad Sci U S A **110**(51): 20777-20782.

Zhang, D. X. and W. B. Levy (1992). "Ketamine blocks the induction of LTP at the lateral entorhinal cortex-dentate gyrus synapses." Brain Res **593**(1): 124-127.